J. Physiol. (1984), **357**, *pp.* 575–607
With 15 text-figures
Printed in Great Britain

THE PHOTOCURRENT, NOISE AND SPECTRAL SENSITIVITY OF RODS OF THE MONKEY *MACACA FASCICULARIS*

BY D. A. BAYLOR, B. J. NUNN* AND J. L. SCHNAPF

From the Department of Neurobiology, Sherman Fairchild Science Building, Stanford University School of Medicine, Stanford, CA 94305, U.S.A.

(*Received 21 March 1984*)

SUMMARY

1. Visual transduction in rods of the cynomolgus monkey, *Macaca fascicularis*, was studied by recording membrane current from single outer segments projecting from small pieces of retina.

2. Light flashes evoked transient outward-going photocurrents with saturating amplitudes of up to 34 pA. A flash causing twenty to fifty photoisomerizations gave a response of half the saturating amplitude. The response–stimulus relation was of the form $1-e^{-x}$ where x is flash strength.

3. The response to a dim flash usually had a time to peak of 150–250 ms and resembled the impulse response of a series of six low-pass filters.

4. From the average spectral sensitivity of ten rods the rhodopsin was estimated to have a peak absorption near 491 nm.

5. The spectral sensitivity of the rods was in good agreement with the average human scotopic visibility curve determined by Crawford (1949), when the human curve was corrected for lens absorption and self-screening of rhodopsin.

6. Fluctuations in the photocurrent evoked by dim lights were consistent with a quantal event about 0·7 pA in peak amplitude.

7. A steady light causing about 100 photoisomerizations s^{-1} reduced the flash sensitivity to half the dark-adapted value. At higher background levels the rod rapidly saturated. These results support the idea that dim background light desensitizes human scotopic vision by a mechanism central to the rod outer segments while scotopic saturation may occur within the outer segments.

8. Recovery of the photocurrent after bright flashes was marked by quantized step-like events. The events had the properties expected if bleached rhodopsin in the disks occasionally caused an abrupt blockage of the dark current over about one-twentieth of the length of the outer segment. It is suggested that superposition of these events after bleaching may contribute to the threshold elevation measured psychophysically.

9. The current in darkness showed random fluctuations which disappeared in bright light. The continuous component of the noise had a variance of about 0·03 pA^2 and a power spectrum that fell to half near 3 Hz. A second component, consisting

* Present address: The Physiological Laboratory, University of Cambridge, Cambridge CB2 3EG.

of discrete events resembling single-photon responses, was estimated to occur at a rate of 0·006 s^{-1}. It is suggested that the continuous component of the noise may be removed from scotopic vision by a thresholding operation near the rod output.

INTRODUCTION

The transduction performed by the retinal rods probably limits many features of scotopic vision. Nevertheless, little is known about the process in the visual system of primates. What information is available comes mainly from psychophysical experiments and recordings of massed electrical signals from the receptor layer of the retina. The work described here analyses the responses to light of single rods of *Macaca fascicularis*. This monkey is thought to have photoreceptors similar to those of man as judged by psychophysical experiments (De Valois, Morgan, Polson, Mead & Hull, 1974) and microspectrophotometry (Bowmaker & Dartnall, 1980; Bowmaker, Dartnall & Mollon, 1980; Dartnall, Bowmaker & Mollon, 1983). With suction electrodes it proved possible to obtain long, stable recordings of the rod photocurrents and to determine a number of the response properties. Brief accounts of some of the work have appeared previously (Nunn & Baylor, 1982, 1983).

METHODS

Animals and surgery

Eyes were obtained from old world cynomolgus monkeys, *Macaca fascicularis*. The animals were imported from Indonesia by commercial suppliers and kept in quarantine for 2 months before use. They were fed Purina monkey biscuits and fruit. Most of the monkeys were donors in heart–lung transplant experiments in the Department of Cardiovascular Surgery at the Stanford Medical School. In addition, four animals were obtained specifically for use in these experiments, so as to better control experimental conditions. The brains of these dedicated animals were taken for neuroanatomical study at the end of the retinal experiments. In setting up the experiments it was useful to carry out trial runs on retinas from the albino rat, which have rods of similar dimensions to those of *Macaca fascicularis*.

In the heart–lung transplant animals enucleation was performed just before removal of the thoracic viscera. Under ketamine and sodium pentobarbitone anesthesia a black plastic occluder was placed over the cornea of one eye and the lids sutured together over it about 20–30 min before enucleation. While the circulation of the eye was still intact the skin at the periphery of the orbit was cauterized and the lids and eye removed *en bloc* with the occluder still in place. The eye was placed in ice-cold Locke solution in a light-tight container and returned to the laboratory for use about 10 min later.

In the dedicated animals the eyes were removed sequentially under full surgical anesthesia. 30 min before enucleation the black occluder was placed over the cornea. Experiments on the cones of the dedicated animals are described elsewhere (Nunn, Schnapf & Baylor, 1984).

Preparation

In the laboratory the eye was cleaned under dim red light (Kodak IA filter). The posterior pole of the eye was cut away with a razor blade and excess vitreous drained from it with tissue paper. Under oxygenated Locke solution the inside of the specimen was examined under infra-red light with an infra-red/visible image converter attached to the dissecting microscope. The composition of the Locke solution was (in mM): Na^+, 140; K^+, 3·6; Ca^{2+}, 1·2; Mg^{2+}, 2·4; Cl^-, 151; HEPES buffer, 3 (pH 7·4); glucose, 10; EDTA, 0·02. After locating the optic nerve head several peripheral pieces of retina, roughly 5–8 mm from the nerve head were cut and isolated into Locke solution or L-15 tissue culture medium (Gibco) and placed in a light-tight container. Under these conditions, cells survived more than 24 h when kept in a refrigerator at a temperature of 5 °C. A piece of retina

was placed receptor-side up and chopped by hand on Sylgard resin or on a Millipore plastic filter with 8 μm pores. The chopped retinal pieces, about 100 μm on a side, were pipetted into a chamber on the stage of a compound inverted microscope equipped with an infra-red light source and an infra-red-sensitive television camera. The chamber was heated to near 37 °C by a glass-insulated Pt wire heater. Purified collagenase (Worthington CLSPA with low tryptic actvity, 0·1–0·5 mg ml^{-1}) was added to the chamber to digest sticky extracellular material. In early experiments the preparation was oxygenated and stirred by blowing moist O_2 on the meniscus at the front of the chamber. In later experiments bicarbonate-buffered Locke solution was continuously perfused through the chamber; this solution contained 20 mM-$NaHCO_3$ (replacing an equal concentration of NaCl). The bicarbonate Locke solution was warmed to 38 °C in a water bath and was continuously bubbled with 95 % O_2/5 % CO_2, which brought the pH to 7·4. The perfusion solution cooled to room temperature as it flowed to the chamber through a 3 ft length of Teflon tubing; on arrival it was rewarmed by a heating wire wrapped around a small glass tube that served as an inlet for the chamber. Photocurrents recorded in the flowing bicarbonate Locke solution were somewhat larger and faster than those in the stirred HEPES Locke solution (see Tables 1 and 4).

Recording

The retinal pieces chosen for study showed a brush of straight outer segments about 25 μm long. Only outer segments unobstructed by other cells were studied so as to minimize unwanted absorption and scatter of the light stimuli. Under visual control the outer segment of a receptor attached to a retinal fragment was drawn into the tip of a glass micropipette coated with silane. The inner diameter of the tip was about 2 μm and the resistance of the electrode 3–10 MΩ without a cell drawn in. From the measured increase in resistance on sucking a cell in, it was estimated that 60–80 % of the current was recorded from the portion of outer segment inside the suction electrode. In making this estimate it was assumed that the resistance of the electrode tip was about half the total electrode resistance, as confirmed in a few cases by measuring the electrode resistance before and after cutting off its tip with a diamond knife. It was often difficult to see the small outer segments after they had been drawn into the pipette, and care had to be taken that only one cell was sucked in at a time. The length of outer segment inside the pipette was often uncertain but sometimes could be gauged from the relative positions of the retinal fragment and electrode tip while drawing the cell in. In different recordings the length in the pipette probably varied between 15 and 25 μm, so that about 40–80 % of the total outer segment current was recorded.

A small calibrated thermistor probe was mounted on the suction electrode a few hundred micrometres from the tip to measure local temperature in the chamber. Tests showed that the thermistor measured the temperature of the solution faithfully when the distal 3 mm was immersed; the retinal pieces were placed in the chamber so that the probe was covered to at least this depth.

Membrane current was measured with a current-to-voltage converter (Baylor, Lamb & Yau, 1979*a*). In perfusion experiments electrical artifacts from the flow were reduced by grounded shields around the inlet and outlet tubing and by a 'bath clamp' that held the voltage of the Locke solution in the chamber at ground potential. Connexions with the current- and voltage-measuring amplifiers were made by Locke-filled bridges and calomel electrodes. The output from the feed-back amplifier of the bath-clamp circuit was connected to the solution with a bare Pt wire or foil. Signals were recorded on a FM tape recorder (Ampex PR-2200). For digitizing the membrane current in the PDP 11/34 computer, the recording was replayed through a six-pole low-pass filter with selectable cut-off frequency.

Light stimuli, rod collecting area and calibration

The stimulus was applied as a spot, 300 μm in diameter, centred on the electrode tip and incident transverse to the long axis of the outer segment. Unless otherwise noted the light was plane polarized with the electric vector at approximately a right-angle to the long axis of the rod. When stimulated in this way an outer segment 25 μm long and 2 μm in diameter, containing rhodopsin at a specific axial density of 0·016 μm^{-1} (e.g. Harosi, 1975) and with a quantum efficiency of isomerization of 0·67 (Dartnall, 1972) should present an effective collecting area, A_c, of 1·9 μm^2 as calculated by eqn. (14) of Baylor, Lamb & Yau (1979*b*). In practice this figure will be an upper limit because the cell dimensions may be somewhat smaller and because the angle of polarization relative to the axis of the cell was not controlled to within better than about 20 deg. Errors in polarization angle have relatively small effects, however; for example, A_c falls by less than 10 %

for an error of 20 deg. When estimating the expected number of isomerizations over an entire outer segment a figure of 1·7 μm^2 will be assumed.

The light was made 'monochromatic' by interference filters with nominal half-widths of 10 nm. The spectral transmission of the filters was measured on a Cary 500 or Perkin-Elmer 330 spectrophotometer. Side-band transmission was found to be negligible by measurements in the spectrophotometer and by visual tests with a dark-adapted eye when other interference or band-pass filters were placed in series with the filter (see Baylor *et al.* 1979*a*). A filter's centre wave-length was taken as that which divided the area under its linear transmission curve in two. The unattenuated irradiance through each filter was measured at the end of the experiment using a United Dectector Technology model 111A radiometer, with the probe placed in the position of the preparation. The power level at any wave-length varied at most by about 2% during a day. A calibrated series of neutral density filters was used to attenuate the stimuli.

Measurement of spectral sensitivity and comparison with psychophysics

The spectral sensitivity was determined relative to the sensitivity at 501 nm using the method of Naka & Rushton (1966) and Baylor & Hodgkin (1973). The relation between flash strength and response amplitude was determined using five or more flash strengths at 501 nm and one to four strengths at other wave-lengths; the average response amplitude was plotted at each wave-length against log photon density and fitted by eye with eqn. (2). The relative logarithmic sensitivities were estimated from the displacements on this scale required to bring the response–stimulus relations into coincidence with the relation at 501 nm. Flashes 100 ms in duration were used in order to permit measurement of the very low sensitivity at long wave-length. (In all other experiments the flash duration was 11 ms.) Several responses at each flash strength were averaged to reduce photon noise, and the response–stimulus relation at 501 nm was determined repeatedly to permit correction for slow changes in the condition of the cell.

The average spectral sensitivity was compared with the psychophysical visibility curve of human scotopic vision after correcting the psychophysical measurements for lens absorption and rhodopsin self-screening. The scotopic visibility curve used for the comparison was that determined by Crawford (1949) using the method of brightness matching. Crawford measured, on an energy basis, the action spectrum of fifty subjects over the wave-length range 380–560 nm, and the spectrum of a further fifty subjects between 480 and 780 nm. The average sensitivities and the variances were recalculated on a quantum basis from Crawford's tabulated results for individual observers. The form of the optical density spectrum of the human lens was obtained from the tabulation by Wyszecki & Stiles (1967); the effect of self-screening by rhodopsin in human rods was calculated by applying Beer's law. An iterative computer program was used to obtain values of lens and rhodopsin densities that made the corrected spectrum for human rods most similar to the spectrum of the monkey rods, as judged by a least-squares criterion. Over the N wave-lengths λ_n in two sets of measurements the program found a minimum for the squared error ϵ calculated according to

$$\epsilon = \sum_{n=1}^{N} [S(\lambda_n) - C(\lambda_n)]^2 / [\sigma_s^2(\lambda_n + \delta_n) + \sigma_c^2(\lambda_n)]. \quad (1)$$

In this expression $C(\lambda_n)$ is the corrected average human sensitivity and $S(\lambda_n)$ the monkey rod sensitivity at wave-length λ_n. Because of slight differences (δ_n) of up to 2 nm between the centre wave-lengths in the two sets of determinations, the values in eqn. (1) for sensitivity of monkey rods at wave-length λ_n were obtained from the measured values by linear interpolation. The terms σ^2 are the variances of the means (sample variance/number of observations) in the original measurements at wave-lengths λ_n and $(\lambda_n + \delta_n)$.

The strength of absorption is expressed by the optical density, defined as $\log_{10}(I_0/I_t)$, where I_0 and I_t are the incident and transmitted light intensities respectively. Wave-length-dependent parameters A_c, k_t and k_s are expressed in terms of their values for a 500 nm photon polarized with the electric vector at right-angles to the rod axis.

RESULTS

Flash responses

Fig. 1 shows a family of superimposed responses to flashes of increasing strength, with the membrane current of the outer segment plotted relative to the level in darkness. Responses to dim flashes were averaged from multiple trials. The

amplitudes of the outward-going photocurrents were graded with the photon density of the flash. The saturating photocurrent, which presumably corresponds to complete suppression of the inward dark current (Penn & Hagins, 1972; Baylor *et al.* 1979*a*), was 34 pA in this rod and varied between cells (Table 1). The dark currents measured here agree with estimates of 18–40 pA from recordings of

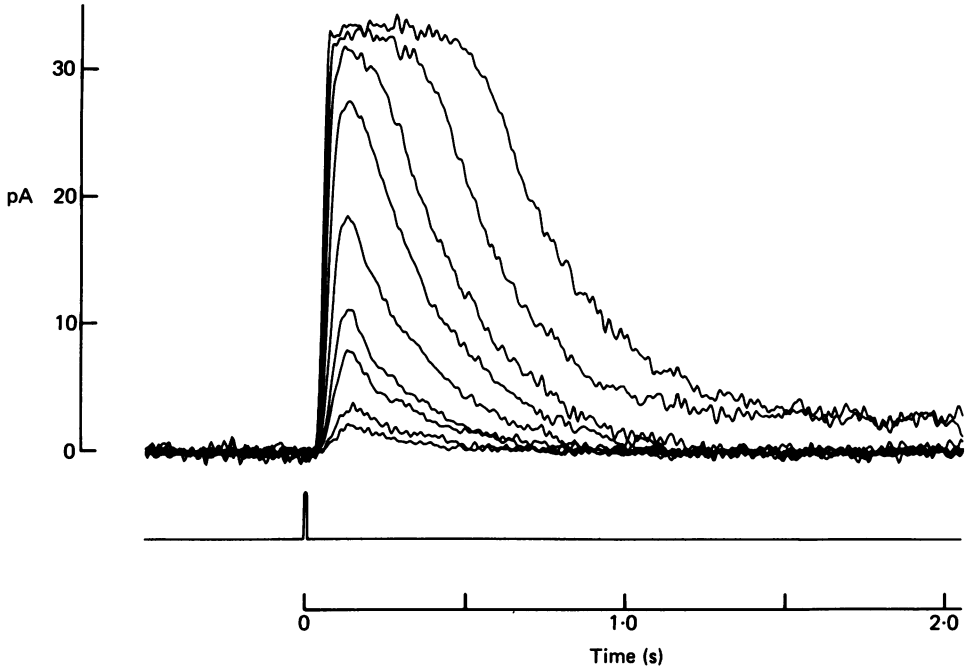

Fig. 1. Family of superimposed responses to 11 ms flashes of increasing strength, with outer segment current plotted relative to dark level (outward change in membrane current plotted upwards). Stimulus timing shown by flash monitor below records. Lower traces averaged from up to six responses, uppermost trace is a single sweep. Flash photon densities raised from 1·7 to 503 photons μm^{-2} at 500 nm. Band width 0–50 Hz, temperature 36 °C, bicarbonate buffer. Cell 7 in Table 1.

massed currents of albino rat rods at the same temperature (Hagins, Penn & Yoshikami, 1970, confirmed by our measurements with suction electrodes). After the two brightest flashes in Fig. 1, the photocurrent showed a long tail 2·5 pA above the dark level. This component of the response is described further on p. 593.

Dependence of response amplitude on flash strength. The variation of peak response amplitude with flash strength is plotted on normalized axes in Fig. 2, which collects results from five rods with large responses. The smooth curve was drawn according to the exponential saturation characteristic (Lamb, McNaughton & Yau, 1981):

$$r/r_{max} = 1 - e^{-k_f i}, \quad (2)$$

where r is the amplitude at the peak of the response, r_{max} the amplitude of the maximal response, i the flash photon density (in photons μm^{-2}) and k_f is a proportionality constant characteristic of the cell. The constant k_f is related to the

half-saturating flash strength, i_0, by $i_0 = (\ln 2)/k_f$. Values of k_f, sensitivity to dim flashes and maximum response amplitude for the cells of Fig. 2 and for other cells with large r_{max} are given in Table 1. The average value of k_f was $0{\cdot}036 \pm 0{\cdot}014$ μm^2 (mean $\pm$ S.D., seven cells in Table 1). Assuming an effective collecting area of $1{\cdot}7$ μm^2 (see p. 578), about thirty isomerizations elicited a half-maximal response, and 200

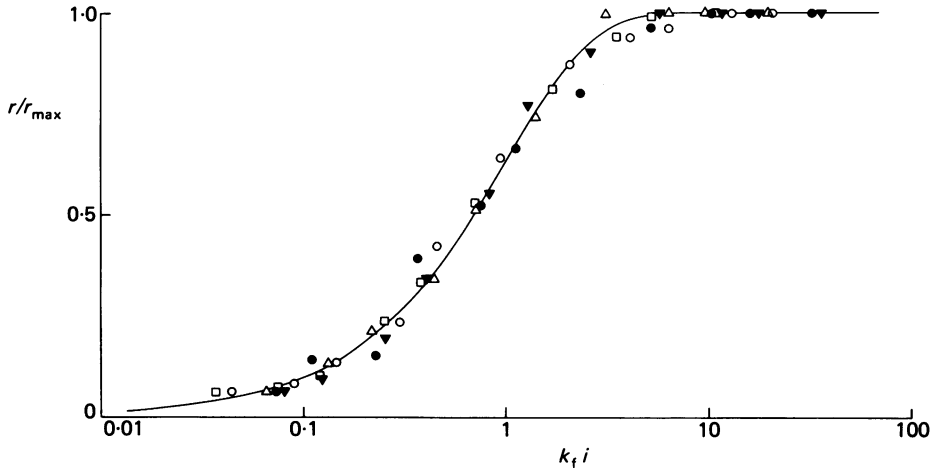

Fig. 2. Relation between normalized photocurrent at the peak of the flash response and normalized flash photon density (logarithmic scale). Collected results from five cells (individual values of r_{max} and k_f given in Table 1). Curve drawn according to eqn. (2) of text.

isomerizations just saturated. Eqn. (2) describes the relation between photon density and response amplitude in toad rods at fixed early times after a flash (Lamb *et al.* 1981), but is steeper than the Michaelis relation which fits the peak amplitudes of responses of toad rods (Baylor *et al.* 1979*a*).

The response would grow toward saturation according to eqn. (2) if each photoisomerization completely suppressed the inward current along a fixed, short length of outer segment and if the length of the blocked region varied with the time course of the observed response (Lamb *et al.* 1981). The constant k_f corresponds to the effective collecting area of the short segment that is blocked by one photon at the peak of the response. This length, Δ, can be calculated by

$$\Delta = Lk_f/A_c, \tag{3}$$

where L is the length of the outer segment and A_c is the effective collecting area of the entire outer segment. For $k_f = 0{\cdot}036$ μm^2, $L = 25$ μm and $A_c = 1{\cdot}7$ μm^2, Δ corresponds to $0{\cdot}53$ μm.

Kinetics of responses to dim flashes. The points in Fig. 3 show the average response of a rod to a series of dim flashes. The continuous curve through the points has the form of the impulse response of the Poisson filter of Baylor, Hodgkin & Lamb (1974). Their eqn. (44) may be rewritten in normalized form as

$$r^*(t) = iS_F^D[\bar{t}\, e^{(1-\bar{t})}]^{n-1}, \tag{4}$$

where $r^*(t)$ is the linear response, i the photon density of the flash (photons μm^{-2}), S_F^D the flash sensitivity (pA photon^{-1} μm^2), n the number of delay stages and $\bar{t}$ time after the flash normalized by the time to the peak ($\bar{t} = t/t_{peak}$). The smooth curve of Fig. 3 was drawn according to eqn. (4) with $n = 6$ and $t_{peak} = 200$ ms. The response to dim flashes was usually fitted by the Poisson model with $n = 6$. Flash responses

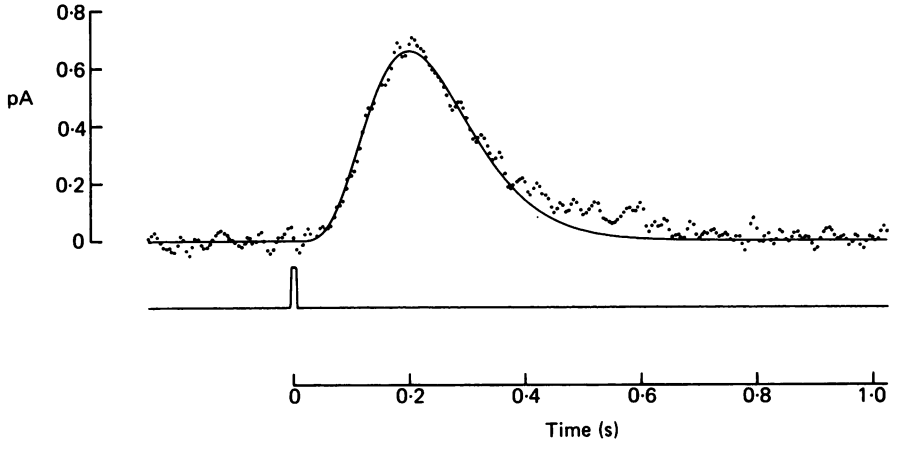

Fig. 3. *A*, average of 264 responses to dim flashes (points). Smooth curve is impulse response of six identical low-pass filters in series (eqn. (4), $n = 6$, $t_{peak} = 200$ ms). Recording temperature 36 °C. Saturating response 22 pA; flashes 0·58 photons μm^{-2} at 500 nm and 11 ms in duration. Band width 0–50 Hz. Bicarbonate buffer. Cell 5 in Table 1.

recorded from some rods were more asymmetric than that in Fig. 3 and were better described by the independent activation model of Baylor *et al.* (1974) with the same number of delay stages (Table 1). Both models, however, often provided only an approximate description of the responses, as the wave form frequently displayed an additional slow component on the falling phase. This feature, evident in the response of Fig. 3, and even more prominent in responses of some other cells, could not be fitted by any adjustment of the time constants in the multi-stage filter models.

For rods in bicarbonate-buffered Locke solution, t_{peak} of the response to a dim flash was 190 ± 38 ms (mean $\pm$ S.D., eighteen cells in Tables 1 and 4). In HEPES buffer, the responses were slower, although the form could still be approximated by a six-stage filter model. For the eight cells in HEPES in Tables 3 and 4, t_{peak} was 281 ± 38 ms. Comparable values were reported for rat rods at similar temperatures ($t_{peak} = 200$–400 ms, Penn & Hagins, 1972). The larger values of t_{peak} for toad rods ($\geqslant 1$ s, Baylor *et al.* 1979*a*) are attributable to the lower recording temperature (see Discussion).

The integration time t_i of the dim-flash response was determined by measuring the area under the response and dividing it by the peak response amplitude (Baylor & Hodgkin, 1973). For the cells in bicarbonate, t_i was 275 ± 65 ms (mean $\pm$ S.D., eleven cells in Tables 1 and 4). Cells in HEPES buffer had longer integration times (Table 4).

TABLE 1. Response properties of cells with maximal responses, $r_{max} \geqslant 18$ pA. All experiments in bicarbonate Locke solution. S_F^D, flash sensitivity to transverse illumination; t_{peak}, the time from the flash to response peak; t_i, the integration time of the flash response; form, the model best fitting the flash response (I = independence; P = Poisson; number in parentheses = number of stages); a, peak amplitude of single-photon response measured by the ratio of variance to mean of flash response (v), or by the fit of amplitude histogram to a Poisson distribution (h); A_c, the collecting area for transverse illumination obtained from S_F^D/a, where a was calculated from the variance to mean ratio (v), from the fit of the response histogram (h), or by fitting eqn. (6) to the 'frequency of seeing' results (s); k_f, obtained by fitting eqn. (2) to response–intensity relation; T, temperature

Cell	Figure (symbol)	r_{max} (pA)	S_F^D (pA photons^{-1} μm^2)	t_{peak} (ms)	t_i (ms)	Form (stages)	a (pA)	A_c (μm^2)	k_f (μm^2)	T (°C)
1	2 (▼)	22	0·51	238	358	I (6)	0·43 (v)	1·16 (v)	0·0296	35
2	—	21	0·66	260	341	P (6)	0·93 (v)	0·71 (v)	0·0478	35
3	2 (●)	25	1·28	216	288	I (6)	0·69 (v)	1·85 (v)	0·0613	36
	—	—	—	—	—	—	0·88 (h)	1·50 (h)	—	—
4	—	18	0·84	200	—	—	0·97 (h)	0·86 (h)	—	38
5	2 (△), 3, 10,	22	1·26	200	269	P (6)	0·95 (v)	1·34 (v)	0·0365	36
	13*A*, 15	—	—	—	—	—	0·97 (h)	1·31 (h)	—	—
6	11, 12	18	1·54	150	—	—	—	—	0·0262	36
7	1, 2 (□)	34	1·17	150	—	—	—	—	0·0217	36
8	—	20	0·46	250	280	—	0·29 (h)	1·57 (h)	—	36
9	—	25	0·55	160	331	—	0·46 (h)	1·19 (h)	—	37
10	—	25	0·70	180	374	—	0·48 (h)	1·47 (h)	—	37
11	2 (○)	27	1·02	150	—	—	—	—	0·0262	37
12	8 (□)	24	0·93	190	330	I (6)	0·75 (v)	1·39 (s)	—	36
	—	—	—	—	—	—	0·76 (h)	—	—	—
13	8 (○)	20	0·58	150	228	P (6)	0·52 (h)	1·33 (s)	—	36
14	8 (△)	23	0·40	150	176	P (6)	0·29 (h)	1·20 (s)	—	35
15	8 (▽)	24	0·68	188	227	P (6)	0·63 (h)	1·14 (s)	—	36

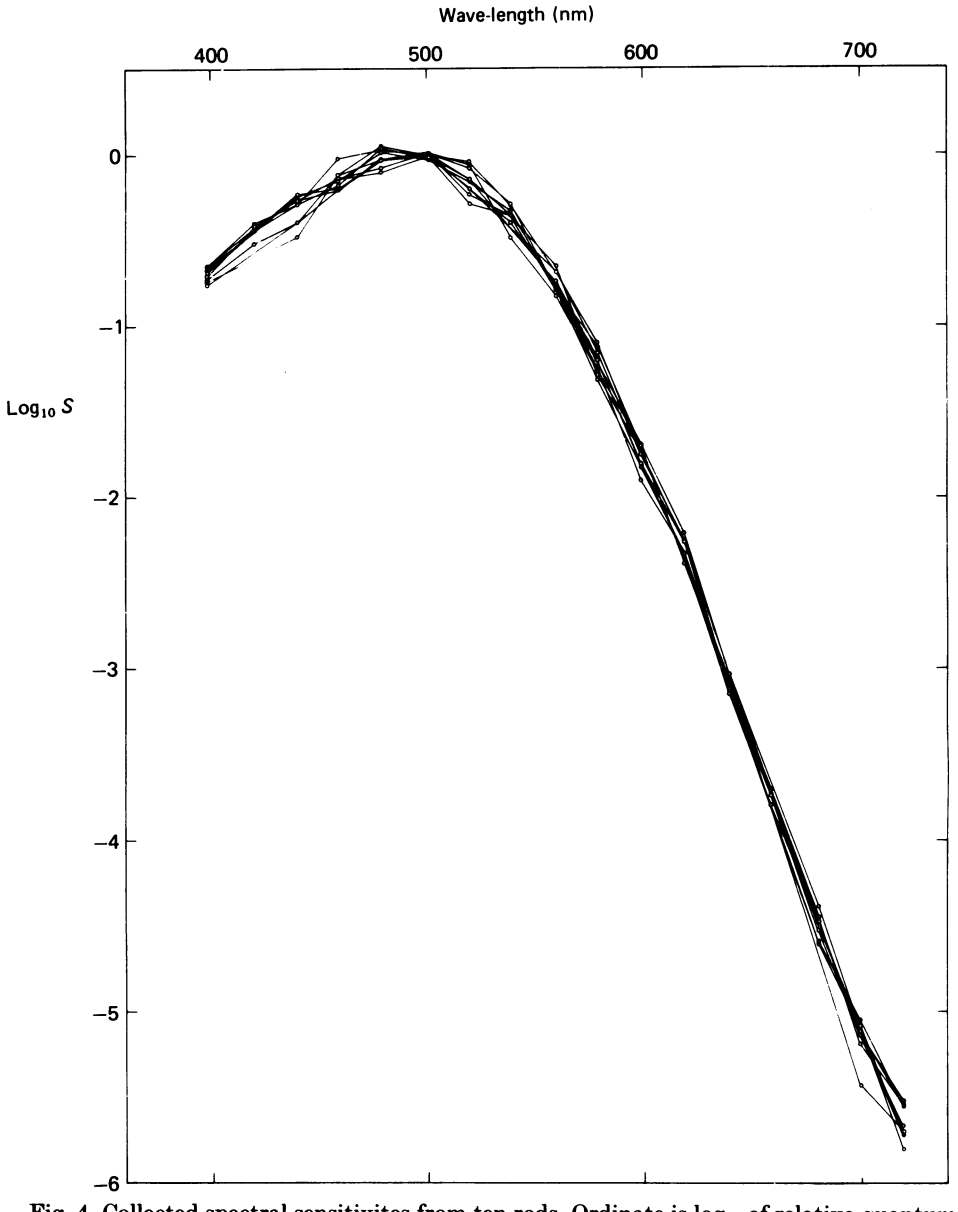

Fig. 4. Collected spectral sensitivites from ten rods. Ordinate is $\log_{10}$ of relative quantum sensitivity, abscissa wave-length. Sensitivities determined as described in Methods. Lines drawn to connect experimental points.

Spectral sensitivity

Normalized action spectra from ten rods of three animals are collected in Fig. 4. Each spectrum was determined relative to the value at 501 nm (see Methods, p. 578) and the individual curves then displaced vertically to minimize the differences between them. The curves from different cells are in close agreement with one another

and show a peak sensitivity near 500 nm. For transverse illumination of a 2 μm diameter outer segment containing rhodopsin at a specific density of 0·016 μm^{-1} (Harosi, 1975; Bowmaker *et al.* 1980), self-screening is negligible. The measured spectrum should therefore be proportional to the molecular extinction coefficient of the rhodopsin. The average normalized spectrum from the rods of Fig. 4 is given in

TABLE 2. Spectral sensitivities. λ is the wave-length, log S the average value of $\log_{10}$ relative sensitivity, S.D. the standard deviation of the log sensitivity, n the number of cells studied at each wave-length. Results from the ten rods of Fig. 4

λ (nm)	Log S	S.D.	n
398	−0·697	0·039	9
420	−0·436	0·039	7
440	−0·314	0·083	9
459	−0·146	0·057	10
479	−0·017	0·049	10
501	0·000	0·015	10
520	−0·151	0·079	10
539	−0·356	0·065	8
560	−0·749	0·060	10
579	−1·220	0·077	9
599	−1·755	0·068	10
619	−2·312	0·058	9
640	−3·093	0·039	10
659	−3·743	0·032	5
681	−4·503	0·070	9
700	−5·147	0·107	10
720	−5·657	0·102	9

Table 2, together with the standard deviation, S.D., of the sensitivity at each wave-length. The standard deviation is least at 501 nm because the method involved measuring the sensitivity at 501 nm repeatedly during each experiment (see Methods).

Estimate of peak sensitivity. The wave-length of maximal sensitivity, λ_{max}, was estimated by plotting the averaged spectrum on a wave-number scale and fitting the Dartnall nomogram for a retinal$_1$-based pigment (Wyszecki & Stiles, 1967, p. 584). Fig. 5 shows the measured spectrum, plotted by ○, and the nomogram of λ_{max} = 491 nm (smooth curve). The fit was significantly worsened when the nomogram was shifted laterally by more than ±3 nm, the fit being particularly critical at long wave-lengths. The dashed continuation of the nomogram was drawn by eye and has a slope at low wave number of 15·0 μm.

Comparison with human scotopic sensitivity. The scotopic spectral sensitivities measured psychophysically in the macaque monkey and man are very similar (Blough & Schrier, 1963; Morgan, 1966; De Valois *et al.* 1974). Fig. 5 (●) shows Crawford's (1949) psychophysically determined human scotopic sensitivity curve after correction for a lens absorption of the form tabulated by Wyszecki & Stiles (1967), scaled to an optical density of 1·54 at 400 nm (0·160 at 500 nm), and for the self-screening of rhodospin expected from an axial optical density of 0·35 at 500 nm. The optical densities that gave the best agreement between the monkey and corrected human spectra were arrived at by minimizing the value of ϵ, the weighted sum of the squared

differences between the two curves (eqn. (1)). The value of ϵ increased by 10 % when the assumed lens density at 400 nm was varied by $\pm 0{\cdot}08$ or when the axial rhodopsin density at 500 nm was changed by $\pm 0{\cdot}06$, so that the fit remained good for assumed lens densities of 1·42–1·62 and rhodopsin densities of 0·29–0·41. These densities for rhodopsin are roughly similar to the value of 0·40 expected for longitudinal

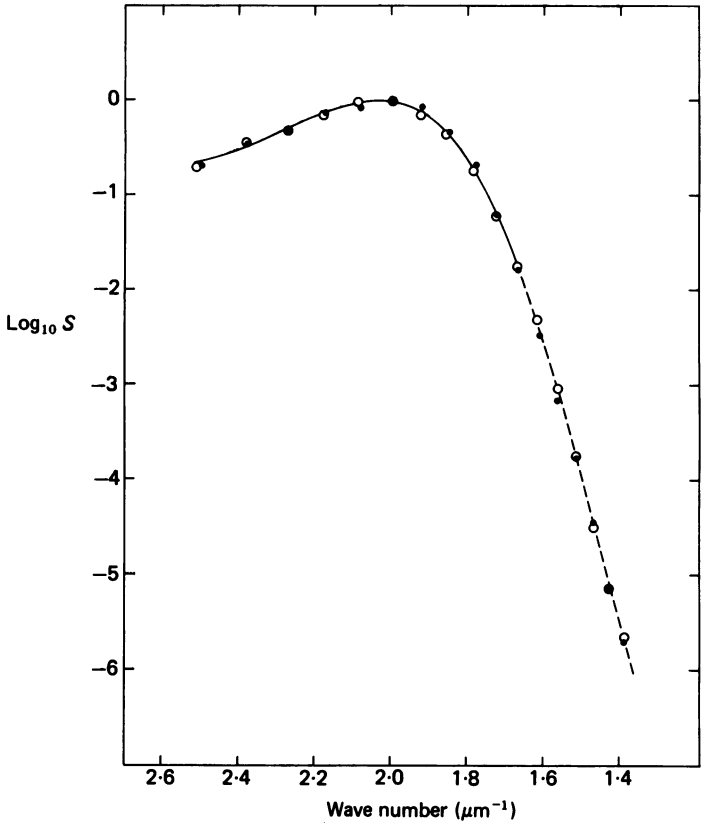

Fig. 5. Comparison of averaged spectral sensitivity of monkey rods (○) with corrected human scotopic sensitivity curve of Crawford (1949, ●) and Dartnall nomogram for rhodopsin with peak absorption at 2·04 μm^{-1} (continuous smooth curve). Crawford's results corrected as described in the text for absorption in the lens and self-screening of rhodopsin. Dashed continuation of nomogram drawn by eye.

illumination of an outer segment 25 μm long with a specific axial density of 0·016 μm^{-1}, and include the range 0·32–0·34 obtained from recent densitometric and psychophysical measurements on humans (Alpern & Pugh, 1974; Zwas & Alpern, 1976). Without correction, the human spectrum coincided closely with the monkey results at long wave-lengths, where lens absorption and rhodopsin self-screening are negligible. Between 640 nm and 720 nm both curves fell approximately along straight lines; the linear-regression slope of log S on $1/\lambda$ was 15·0 μm for the spectrum of *Macaca* rods compared with 14·8 μm for the curve of human scotopic vision.

Single-photon responses

In this section the fluctuations in the photocurrents evoked by dim lights are analysed to determine the properties of the underlying events.

Responses to dim flashes. Fig. 6*A* shows apparent 'failures' and quantal events in the current recorded from a cell during exposure to a series of dim flashes (0·6 photons μm^{-2} at 501 nm). Ignoring dispersion of event amplitudes and assuming linear summation, the unit event amplitude a can be estimated from the ratio of the ensemble variance increase and the amplitude of the average dim-flash response (see Baylor *et al.* 1979*b*). From 116 trials this ratio was 0·68 pA for the cell of Fig. 6, and $0{\cdot}72 \pm 0{\cdot}16$ pA (mean $\pm$ S.D.) for nine cells in Tables 1 and 3. An independent estimate of the event amplitude was obtained from the histogram of peak response amplitudes for the 116 trials, shown in Fig. 7*A*. The response amplitudes were estimated by scaling the amplitude of the ensemble average response to make the best 'least-squares' fit to each sweep (Baylor *et al.* 1979*b*). The form of this histogram reflects the distribution of failures and responses and the dispersion of the peak amplitudes. Assuming that the flash response is indeed quantized and that the occurrence of quantal events in a trial is Poisson distributed, the mean number of responses per flash, m, can be estimated from $-\ln p_0$, where p_0 is the fraction of failures. The estimated unit response amplitude, a, is then given by

$$a = \frac{\mu}{m}, \tag{5}$$

where μ is the mean response amplitude. In order to estimate p_0, the amplitude dispersion of the current in darkness was measured by the least-squares procedure, in which the average flash response was scaled to fit the sweeps in darkness. The dark amplitude histogram obtained in this manner is plotted in the inset of Fig. 7*A* and is similar to the Gaussian curve drawn near the experimental results. The standard deviation, σ_0, of the Gaussian was 0·15 pA (indicated by the arrow). The smooth curve in the lower histogram of Fig. 7*A* was drawn for a Poisson distribution of events; a value of 0·7 for m was found to give the best fit of the theoretical curve to the failures peak, given the base-line dispersion of 0·15 pA. The mean amplitude of the unit response, a, was calculated as 0·68 pA from eqn. (5) with $\mu = 0{\cdot}47$ pA, in agreement with the value of 0·7 pA estimated by eye from the experimental histogram. A value of 0·3 pA was chosen for the dispersion of the unit event amplitude to get the best fit of the remainder of the histogram to the theoretical curve (see Baylor *et al.* 1979*b*, eqn. (10)). The calculated and experimental histograms are in satisfactory agreement, supporting the idea that the response to dim flashes consisted of a Poisson-distributed number of unit responses each around 0·7 pA in amplitude.

Flash response histograms from three other rods are shown in Fig. 7*B–D*. These were measured and fitted with smooth curves as described above, after estimating the dispersion of the base-line from 'dark-noise' histograms (insets). In each case a Poisson distribution of unit events provided a reasonable fit to the experimental histogram. Details of the experiments are given in Table 3. The mean unit amplitude estimated from amplitude histograms was $0{\cdot}65 \pm 0{\cdot}23$ (mean $\pm$ S.D., fourteen cells; Tables 1 and 3), close to the mean value of 0·72 estimated from the ratio of ensemble variance to mean response.

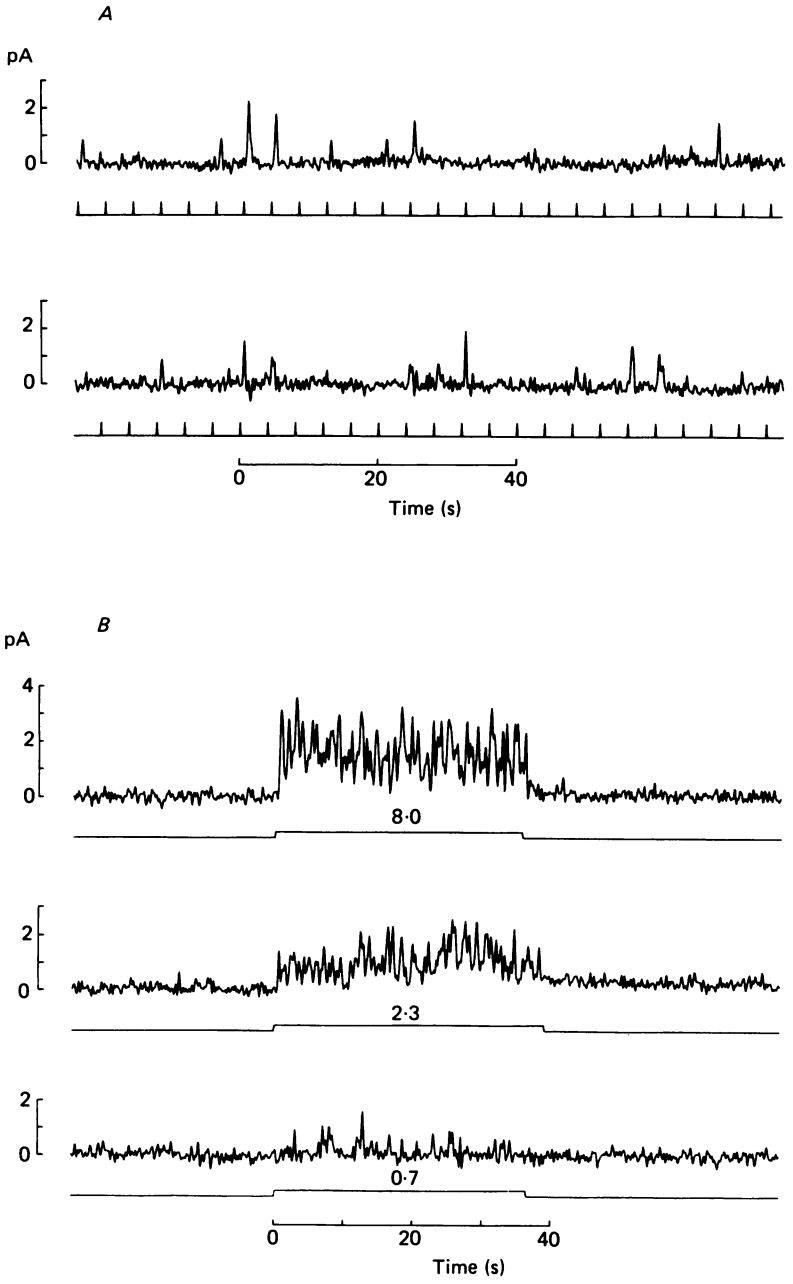

Fig. 6. Photon noise in dim diffuse lights. *A*, responses to fifty-one flashes at 4 s intervals (timing shown by lower traces). Photon density 0·6 photons μm^{-2} at 501 nm. Average response and variance at peak 0·47 pA and 0·32 pA^2 respectively; mean number of responses per flash 0·70 (see text). *B*, responses of same rod to steady light of increasing intensity. Numbers above light monitor traces give photon flux density (photons μm^{-2} s^{-1}) at 501 nm. Mean responses and ensemble variances were, from below: 0·162 pA and 0·059 pA^2; 0·938 pA and 0·278 pA^2; 1·68 pA and 0·494 pA^2. Integration time of flash response 300 ms. Band width 0–3 Hz in *A* and *B*, records in *A* corrected for instrumental drift of $-0·004$ pA s^{-1}.

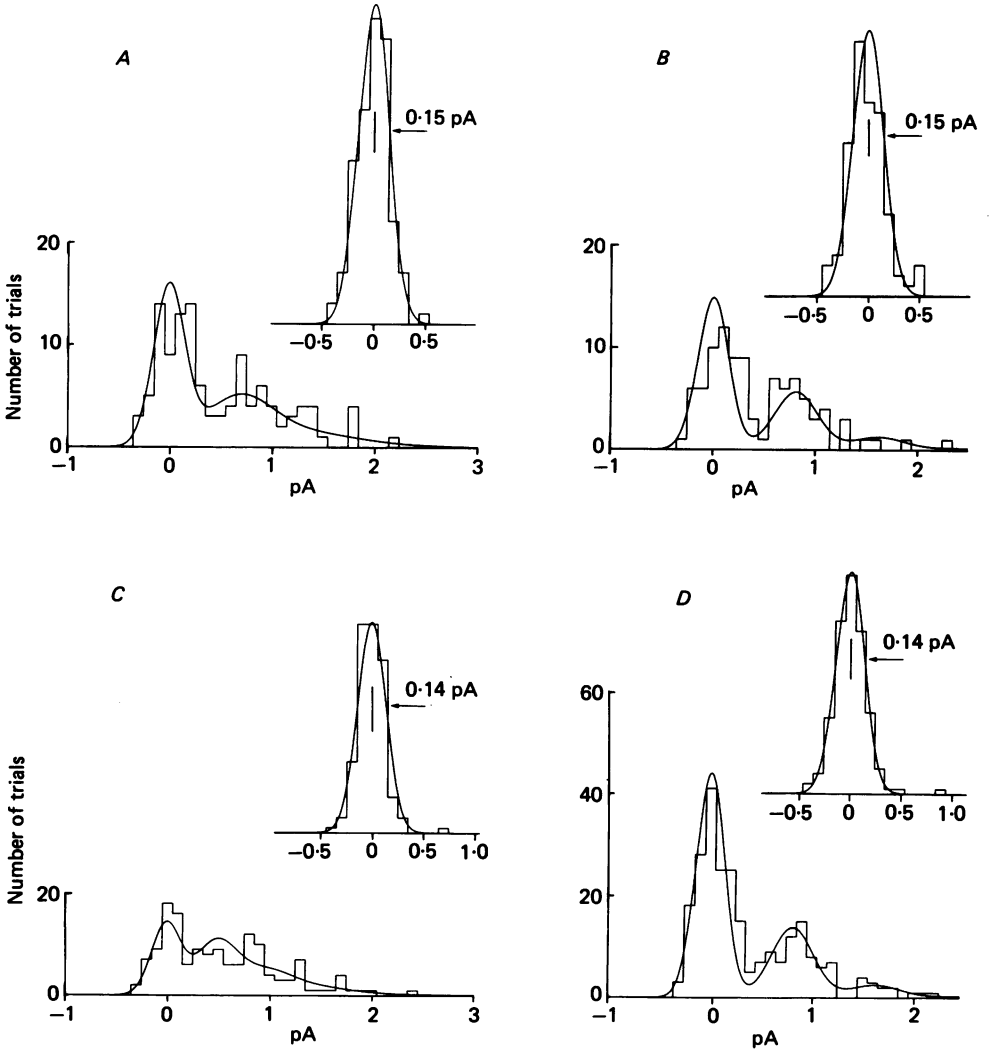

Fig. 7. Amplitude histograms of flash responses from four cells. Ordinate is number of occurrences of response amplitudes shown on abscissa; bin width 0·1 pA. Insets are amplitude histograms for interleaved trials in complete darkness; smooth curves in insets are Gaussians with standard deviation, σ_0 (pA) shown alongside. Smooth curves in lower response histograms drawn assuming a Poisson distribution of events, a base-line noise with standard deviation σ_0, a mean unit event amplitude, a, dispersion of unit event amplitude, σ_1, and mean number of events per trial, m. Details of cells in Table 3; cell in *A* same as in Fig. 6.

In toad rods there is a systematic difference in the amplitude of the quantal response elicited at different positions along the outer segment (Schnapf, 1983). It is possible that some of the amplitude dispersion in the unit event of monkey rods (Table 3) also resulted from longitudinal differences.

The collecting area can be derived from the amplitude histogram by dividing the

estimated mean number of isomerizations per flash, m, by the photon density of the flash. For the cell of Fig. 7*A* this gave the collecting area as 1·2 μm^2. For nine cells in Tables 1 and 3, the collecting area was 1·4 ± 0·53 μm^2 (mean ± S.D.). The collecting area measured in this way depends on the length of the outer segment effectively inside the suction electrode, and this probably varied between 15 and 25 μm in different experiments. Lower values of collecting area may have been derived from recordings over only part of the outer segment length or from cells with somewhat smaller dimensions.

TABLE 3. Response properties of cells in Fig. 7. Figure indicates the Figure in which results from the cell are illustrated, m is the mean number of events per trial used in fitting the histogram, a the mean amplitude of the unit event. A_c is the effective collecting area obtained from the flash histogram (h), the variance-to-mean ratio (v), or from photon noise with dim steps of light (n). σ_0 is the standard deviation of the current in darkness and σ_1 the standard deviation of the unit amplitude. A_c was measured with diffuse 501 nm plane-polarized light. Temperatures 32–38 °C. All cells recorded in HEPES buffer

Figure	m	a (pA)	A_c (μm^2)	σ_0 (pA)	σ_1 (pA)
7*A*	0·70	0·68 (h)	1·17 (h)	0·15	0·30
		0·68 (v)	1·15 (v)	—	—
		0·46 (n)	2·16 (n)	—	—
7*B*	0·54	0·81 (h)	0·72 (h)	0·15	0·20
		0·70 (v)	0·82 (v)	—	—
7*C*	1·1	0·49 (h)	2·57 (h)	0·14	0·15
		0·56 (v)	2·25 (v)	—	—
7*D*	0·46	0·81 (h)	—	0·14	0·15
		0·77 (v)	—	—	—

Frequency of seeing experiments. As a test of the idea that the unitary photocurrent is evoked by isomerization of a single rhodopsin molecule, 'frequency of seeing' experiments (Hecht, Shlaer & Pirenne, 1942; Fuortes & Yeandle, 1964; Scholes, 1965; Baylor *et al.* 1979*b*) were performed on four rods. This kind of experiment also gives a better estimate of the effective collecting area and provides a check on the calibration of the absolute intensity of the stimuli.

The rationale of the experiment is that if the unitary response is triggered by a single photoisomerization, then the probability p_s that a flash of photon density i will give at least one unitary response should be

$$p_s = 1 - e^{-A_c i}, \tag{6}$$

where A_c is the effective collecting area of the outer segment. The points in Fig. 8 show the fraction of successes in multiple trials as a function of flash strength (logarithmic scale). Successes and failures were estimated from response-amplitude histograms prepared from fifty-nine to seventy-three trials; each kind of symbol shows results from a different cell. The continuous curve was drawn according to eqn. (6) with a value of the collecting area equal to 1·26 μm^2, as compared to the expected figure of 1·7 μm^2 (p. 578). Better agreement probably would not be expected given the uncertainties in the effective length of outer segment recorded from. The hypothesis that two or more isomerizations were required to evoke a response yielded theoretical curves that were too steep to fit the form of the results; unreasonably large

values for the collecting area were also needed for even a rough fit. For example, assuming that two isomerizations were needed to elicit a response, the curve was already too steep and the best fit to the experimental results required that the collecting area, $A_c = 3\ \mu m^2$. The conclusion is that the quantal electrical response was generated by isomerization of a single rhodopsin molecule.

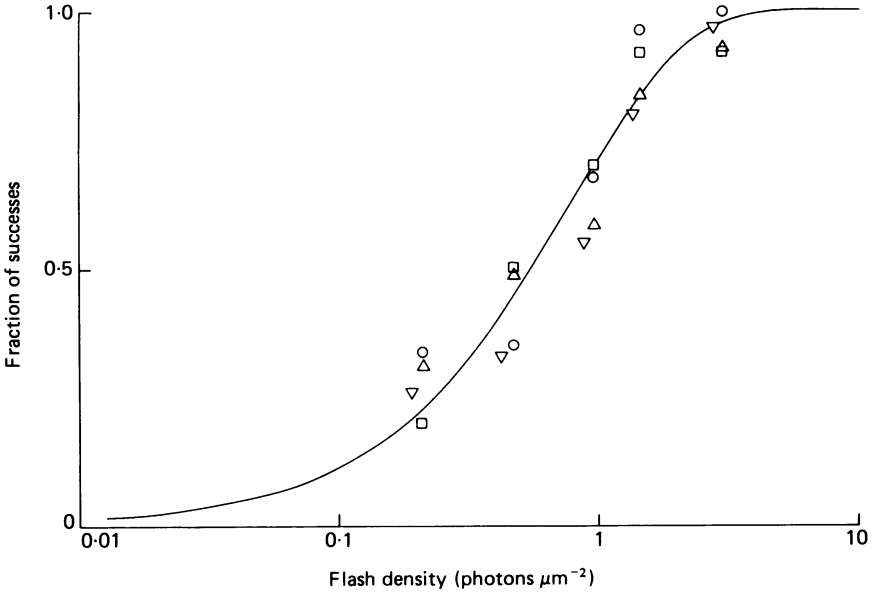

Fig. 8. 'Frequency of seeing'. Collected results from four rods. Fraction of trials in which the light flash successfully elicited a response plotted as a function of the photon density of the flash on a logarithmic scale. Smooth curve drawn according to eqn. (6) with $A_c = 1{\cdot}26\ \mu m^2$. Each point derived from amplitude histograms calculated from fifty-nine to seventy-three responses. Flashes 11 ms, 500 nm. Bicarbonate buffer. Cells 12–15 in Table 1.

Analysis of fluctuations in dim steady light. Several results from previous sections can be confirmed and extended by examination of the current fluctuations evoked by dim steady light. Analysis of the fluctuations gives independent estimates of the size of the single-photon effect and the collecting area of the outer segment. Tests were also made of the notion that the response to steady light simply consists of a Poisson stream of linearly additive unitary events.

Current fluctuations evoked by steady lights of three intensities are illustrated in Fig. 6*B*. In the dimmest light the resonse appeared to consist of isolated shot events. Assuming that such events occur randomly and independently in time, have a fixed size and shape and sum linearly, the event amplitude a is given by $s\sigma^2/\mu_s$, where s is a shape factor characteristic of the event, σ^2 is the variance increase, and μ_s is the mean amplitude of the steady response (Katz & Miledi, 1972). In applying this to determine the event amplitude, it was assumed that the shape of the event was the same as the shape of the average response to a dim flash. The flash response of the rod of Fig. 6 was fitted by eqn. (4) with $n = 5$; the shape factor for this response

is 1·43. For the three records of Fig. 6*B* the unit event amplitude was estimated as 0·52, 0·42 and 0·42 pA (from below upward), similar to estimates derived from the flash response analysis.

If each unitary event in steady light results from photoisomerization of a single rhodopsin molecule, and if the events sum linearly, the apparent collecting area, A_c, can be calculated from the intensity, I_s, of the steady light by the formula

$$A_c = \frac{\mu_s}{a t_i I_s}. \tag{7}$$

For the cell of Fig. 6*B*, where t_i was 0·3 s, the average collecting area estimated in this way was 2·2 μm^2. A value of 1·2 μm^2 was obtained from analysis of the flash response (Fig. 7*A*) and a value of 1·7 μm^2 is expected (p. 578). Therefore, the response to dim steady light was roughly as expected for a superposition of random photon responses.

Effect of background light on flash sensitivity

The variation of response amplitude with flash strength exhibited an exponential saturation described by eqn. (2). This section shows that the desensitizing effect of background light was largely explained by the same saturation, preceded by a linear time-invariant summation of single-photon effects.

On the model of the saturation outlined on p. 580 one photon blocks a short length Δ of the outer segment for a mean time t_i; the collecting area of a length Δ is k_f. In a steady light of intensity I_s there will be an average of $k_f t_i I_s$ photons acting on each short length at any instant and the fraction of lengths remaining unblocked will be $e^{-k_f t_i I_s}$. The flash sensitivity S_F in background light, relative to the value S_F^D in darkness, should then be

$$S_F / S_F^D = e^{-k_s I_s}, \tag{8}$$

where $k_s = k_f t_i$.

Fig. 9 plots on normalized axes the variation of flash sensitivity with background intensity from seven rods. The test flashes were adjusted to evoke responses in the linear range, and the sensitivity was estimated from ten to fifteen trials in order to reduce photon noise. The values of k_s used to scale the intensities of the background light for each experiment were calculated as the product of the parameters k_f and t_i derived from responses to flashes presented in darkness. The average value of k_s was 0·0158 μm^2 s for all seven cells studied, and 0·0123 for the three in bicarbonate (Table 4). The flash sensitivity of the cells in bicarbonate was reduced to half the dark-adapted value by about 60 photons $\mu m^{-2} s^{-1}$, or about 100 isomerizations s^{-1}. The smooth curve in Fig. 9 was drawn according to eqn. (8) and provides a reasonable description of the experimental results, suggesting that the densitizing effect of steady light resulted mainly from response saturation. Consistent with this there was little decline in the response to a bright step and little if any shortening in the time scale of flash responses in background light. The maximum reduction in t_{peak} and t_i was by about 1·4 times (Table 4). This is quite different from the behaviour of turtle cones (Baylor & Hodgkin, 1973) and toad rods (Baylor *et al.* 1979*a*), where background light reduces the time to peak of the dim-flash response by as much as a factor of three.

The characterization of the transduction as a linear time-invariant filter followed

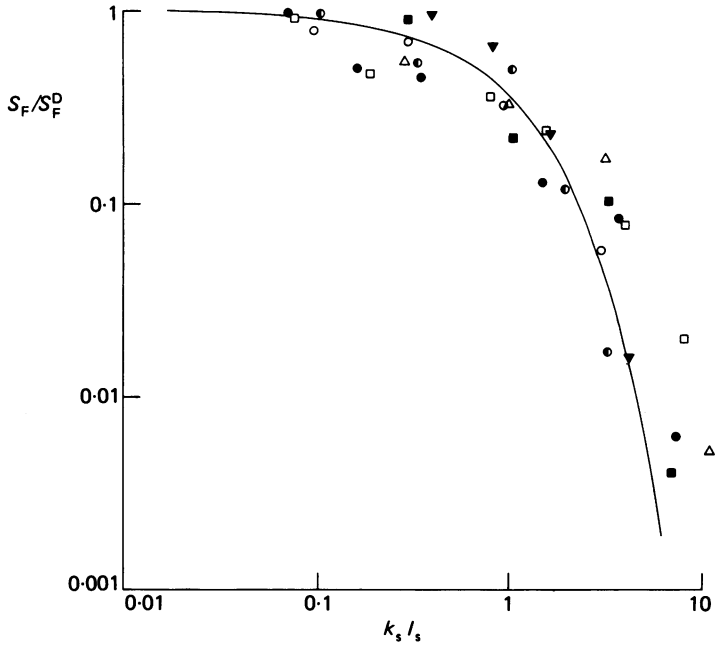

Fig. 9. Relative flash sensitivity plotted against the scaled background intensity, $k_s I_s$. Values of k_s determined from measurements in the dark-adapted state; S_F^D averaged from measurements before and after each run in steady light. Collected results from seven cells. Cell details in Table 4. Smooth curve drawn according to eqn. (8).

TABLE 4. Response properties of cells in Fig. 9. Values of S_F^D and k_f are given as expected for 500 nm light, plane-polarized with the electric vector transverse to the rod axis; t_{peak}, t_i and k_f measured without background light. f is the maximum factor by which background light reduced the integration time of the incremental flash response. Buffer: H = HEPES, B = bicarbonate. Cells 5–7 were stimulated with unpolarized light and measured values of k_f and S_F^D were multiplied by 1·5 to obtain the values in the table. Temperatures 34–36 °C

Cell	Symbol	r_{max} (pA)	S_F^D (pA photons^{-1} μm^2)	t_{peak} (ms)	t_i (ms)	k_f (μm^2)	f	Buffer
1	◐	10	0·51	265	292	0·0529	1·01	H
2	○	14	0·54	250	300	0·0468	1·13	H
3	△	18	0·74	250	333	0·0653	1·40	H
4	■	10	0·39	300	400	0·0562	1·19	H
5	▼	11	0·19	150	175	0·0690	1·01	B
6	●	11	0·43	220	228	0·0518	1·14	B
7	□	16	0·87	220	248	0·0518	1·40	B

by a saturation is nevertheless an approximation, as the flash response of most rods did shorten slightly in steady light. As a result, the fractional blockage of the outer segment by steady light was less than that expected from the simple saturation model. The effect of the intensity-dependent reduction in t_i is illustrated by the behaviour of cells 3 and 7 in Table 4. For these cells the integration time in darkness divided by the minimum value in light was 1·4, and consistent with the shortened integration times the sensitivities measured in bright light lie to the right of the theoretical curve

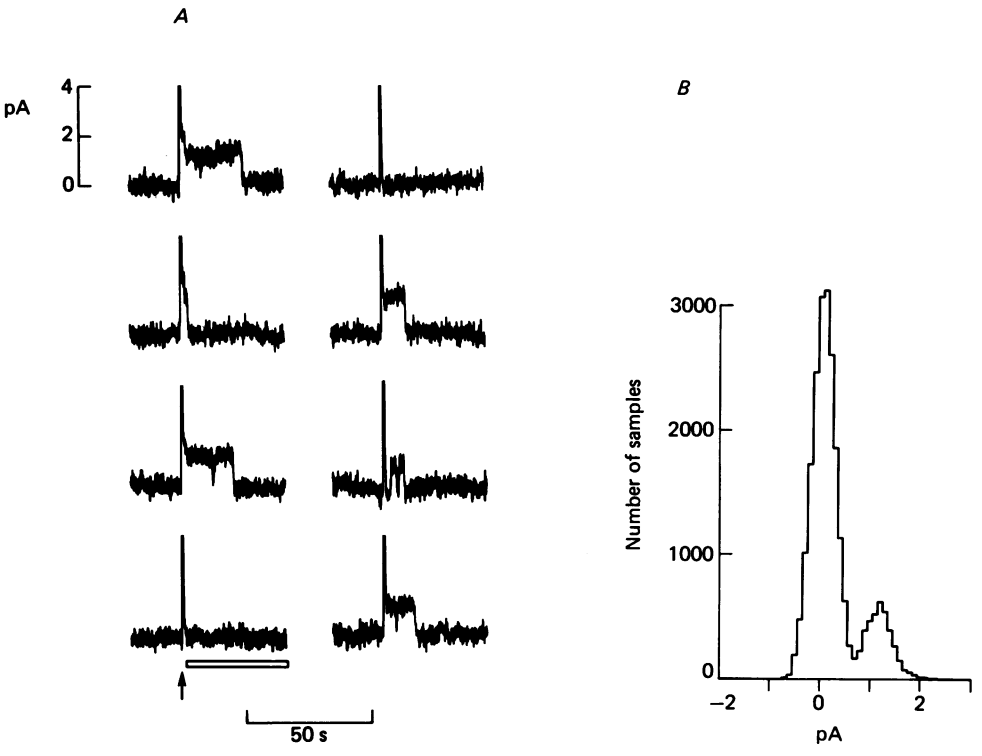

Fig. 10. Stepped recovery after bright flashes. *A*, responses to eight successive flashes at tip of the outer segment. Flash timing shown by arrow. Response peak, 15 pA, truncated. 2·5 μm wide slit of 520 nm light, $2{\cdot}1 \times 10^3$ photons μm^{-2}, causing approximately 250 isomerizations per flash. *B*, scaled probability density of the current amplitude measured over the time window shown by the open bar in *A*. Histogram prepared from seventeen trials, including those shown in *A*. Amplitudes measured relative to the average of the base line before the flash. Sampling interval 30 ms, total number of points 22576. Band width 0–5 Hz. Temperature 36 °C. Cell 5 in Table 1.

(Fig. 9, △, □). On the other hand, the kinetics of the flash response of cells 1 and 5 (Table 4) were unchanged by background light and the relation between background intensity and flash sensitivity was well described by eqn. (8) (Fig. 9, ◐, ▼).

Step-like current transitions evoked by bright light

General features. Fig. 10*A* shows responses to a series of bright flashes delivered locally on the distal third of the outer segment. Each flash was expected to give about 250 photoisomerizations. During recovery of the photocurrent there were step-like current transitions of amplitude 1·2–1·5 pA; similar events occurred after diffuse flashes. We use 'step' to refer to the plateau phase of these events, which were elicited by bright light in every rod examined. Fig. 10*B* shows the probability density of the current amplitude during recovery, as measured in seventeen trials. The histogram was measured over the time window shown in Fig. 10*A*. Quantization of the amplitude is evident, and the size of the event, judged by the distance between the

peaks, is 1·2 pA. From measurements on records from thirty-five cells the step amplitude was estimated as 1·16 ± 0·38 pA (mean ± S.D.).

Several observations indicate that steps were a genuine feature of the response to light rather than an artifact of the method. The measured electrode resistance did not change during an event, so that a step did not result from a change in the efficiency of current collection by the electrode. Although sudden longitudinal movements of the cell within the electrode might give step changes of 1–2 pA, very bright light caused a superposition of multiple steps to an amplitude of more than 10 pA, from which the current tumbled down. The mechanical movement required to give a change of this size is roughly 10 μm, which should have been easily visible. Steps were never observed during the saturating photocurrent, indicating that they represent a reduction in the current through the light-sensitive channels.

The number and duration of the steps varied between trials, and the step amplitude was quantized (Figs. 10*B* and 11*B*). These features are reminiscent of single-channel currents, and by analogy it seems likely that the steps were gated by single molecular transitions. The amplitude of a step, however, is almost certainly too large to be explained by blockage of a single light-sensitive channel (e.g. Detwiler, Conner & Bodoia, 1982). We suppose instead that a step results from blockage of the dark current over a length of roughly 1–2 μm of the outer segment by a local change in the concentration of internal transmitter. On the 'Ca' hypothesis, for example, this might occur if a gating event in a single channel or carrier molecule caused a steady injection of Ca into the cytoplasmic space of the outer segment.

When examined with wide band width on an expanded time base the rise and fall of the steps were not instantaneous but instead occurred in roughly 0·5 s. The transitions had approximately the form of the time integral of the dim-flash response, but they were not well resolved because of the instrumental noise. The random timing of the transitions made averaging difficult.

An alternative way of explaining the steps would be to suppose that they result from intracellular depolarization rather than blockage of the light-sensitive conductance. This seems unlikely for two reasons. First, because the light-sensitive conductance is strongly rectifying (e.g. Bader, MacLeish & Schwartz, 1979), a large depolarization, probably more than 10 mV, would be required to give even a single step. Secondly, evidence to be presented shows that the kinetics of the steps depend on the longitudinal position of light absorption in the outer segment. This parallels a longitudinal variation in the kinetics of bleaching recovery and single-photon responses, suggesting a local blockage of light-sensitive channels (Baylor & Lamb, 1982; Schnapf, 1983).

Superposition of steps. Fig. 11*A* shows the recovery of three responses to flashes expected to give about 3000 photoisomerizations. During return to the dark level the current jumped between several levels. The probability-density histogram in *B* was prepared from these and eighteen other similar trials; measurements were made during the period shown by the bar in Fig. 11*A*. The histogram shows peaks at amplitudes of 0, 1·25 and 2·5 pA, with additional humps near 3·3 and 4·5 pA. The records and the histogram are consistent with the interpretation that the slow tail on the photocurrent consists of a superposition of quantized events of unit amplitude 1·25 pA. In the histogram, the peaks at 3·3 and 4·5 pA are at smaller amplitudes than

expected for linear summation of three and four events respectively, presumably because of amplitude compression. Steps were also evident during recovery from still brighter lights, which evoked longer tails. As a working hypothesis, we assume that the 'after-image signals' which follow bright lights consist of a superposition of steps. Further tests of this notion will require a larger number of trials.

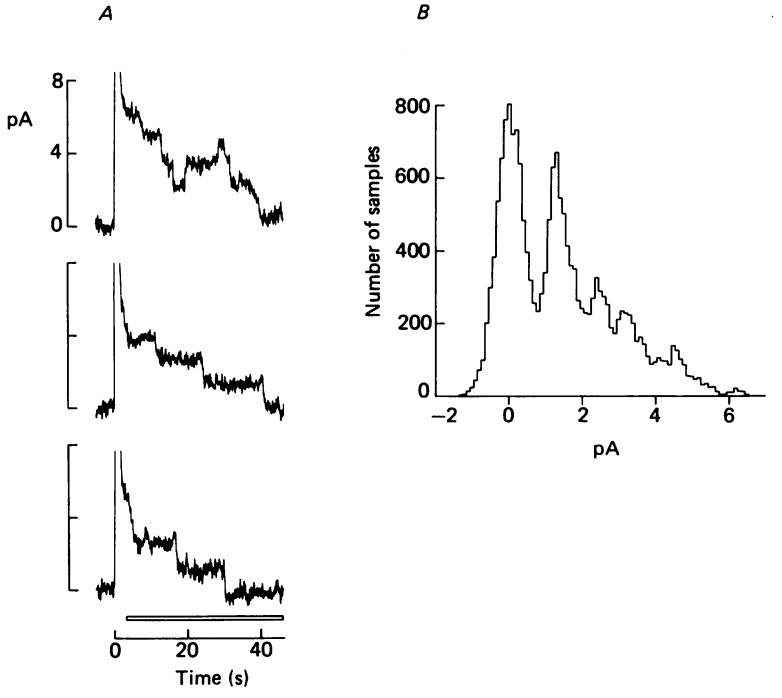

Fig. 11. Superposition of steps after bright flashes. *A*, responses to bright flashes delivered at time $t = 0$, with the peak response of 18 pA truncated. Flashes diffuse and expected to give 2960 photoisomerizations. Band width 0–5 Hz. *B*, scaled probability density histogram of current amplitude from twenty-one trials (three shown in *A*). Histogram measured over window shown by open bar in *A*. In fifteen trials the flash was expected to give 2960 photoisomerizations, in six trials 2220 photoisomerizations. Band width 0–2 Hz, sampling interval 50 ms. Amplitude of each point in sampling window measured relative to average initial base line before flash. Total number of points 18060. Cell 6 in Table 1.

The reduction in dark current and the increased current noise during the tail may explain the elevation in 'dark light' observed to follow bleaching in psychophysical experiments (e.g. Barlow, 1972).

Dependence of occurrence of steps on light intensity. The probability of occurrence of steps rose with increasing flash strength. It was not practical to determine a complete 'frequency of seeing' curve because of the large number of trials and long inter-trial interval required. Instead, in several cells the average response was calculated from a number of trials at fixed intensity and the amplitude of the tail taken as an index of the average number of steps present. In one rod illuminated with

dim diffuse light the flash strength was varied in four steps between $1{\cdot}07 \times 10^4$ and $2{\cdot}36 \times 10^4$ photoisomerizations. The tail declined approximately along a single exponential of time constant 9 s (8–10 s for different flash strengths) and the amplitude of the tail scaled approximately linearly with flash strength over the limited range examined. This simple behaviour did not continue to hold for brighter lights, which gave progressively slower decays. The apparent linearity needs to be tested further, particularly with dimmer light. Assuming linearity, the mean number of photoisomerizations associated with generation of a single step was estimated from experiments on six cells as ranging between 250 and 2000. These estimates were made by measuring the slope of the relation between average initial tail amplitude and flash strength and then dividing by the step amplitude. Linearity implies that even a very dim flash has a finite probability of triggering a step, and indeed on rare occasions a flash giving only a few photoisomerizations caused a step.

Test of whether steps are triggered by absorption in rhodopsin of disks or surface membrane. Photons absorbed in the outer segment elicited steps with low probability. A possible explanation would be that steps are triggered only by absorption in rhodopsin in the surface membrane. Because the dipole transition moment of rhodopsin is confined to the plane of the membrane in which it lies, the ratio of absorptions in disk and surface membranes will vary with the plane of polarization of the incident light. To examine the site of initiation of steps, three cells were excited by flashes of plane-polarized light whose electric vector was aligned parallel to the long axis of the rod ($\parallel$) or perpendicular to it ($\perp$) (see inset in Fig. 12). The apparent dichroism of disk absorption, expressed by the ratio of sensitivities for the two polarizations, $D = S_\perp/S_\parallel$, was determined by the same procedure used for measuring spectral sensitivity. The light was then brightened to elicit steps and the intensities of the beams adjusted to give approximately equal absorption in the disks for the two planes of polarization. When the intensities are adjusted in this way it can be shown on a simple geometrical basis that absorption in the surface membrane will be greater by a factor of approximately $1{\cdot}5\ D$ for light polarized in the parallel ($\parallel$) orientation. For this adjustment of intensities, parallel polarization ($\parallel$) should be more effective if steps are initiated in the surface, while if they arise from absorption within disks the two polarizations will be equally effective.

Fig. 12 shows averaged responses to bright flashes of polarized light; the long tails of the responses were comprised of steps, as illustrated by the individual sweeps in Fig. 11. Record *A* was with perpendicular polarization ($\perp$, see inset) at a flash strength of $1{\cdot}7 \times 10^3$ photons μm^{-2}. Records *B* and *C* were with parallel polarization ($\parallel$) at flash strengths of $1{\cdot}3 \times 10^3$ and $4{\cdot}0 \times 10^3$ photons μm^{-2} respectively. As the apparent dichroic ratio *D* of disk absorption was 3·05 for this cell, the disk absorptions in records *A* and *C* were similar, and the tails of the responses were also similar. The flashes in record *B* were weaker for the disks but stronger for the surface membrane, and the response tail was very small. This result indicates that absorption of light by rhodopsin of the disks is responsible for initiating steps. Similar results at other flash strengths were obtained from this cell and from two other rods with dichroic ratios of 3·01 and 2·09.

Dichroic ratios ranging from 2·09 to 4·1 were observed in a total of five cells, with a mean of 2·99. A value of about four is expected from results with microspectro-

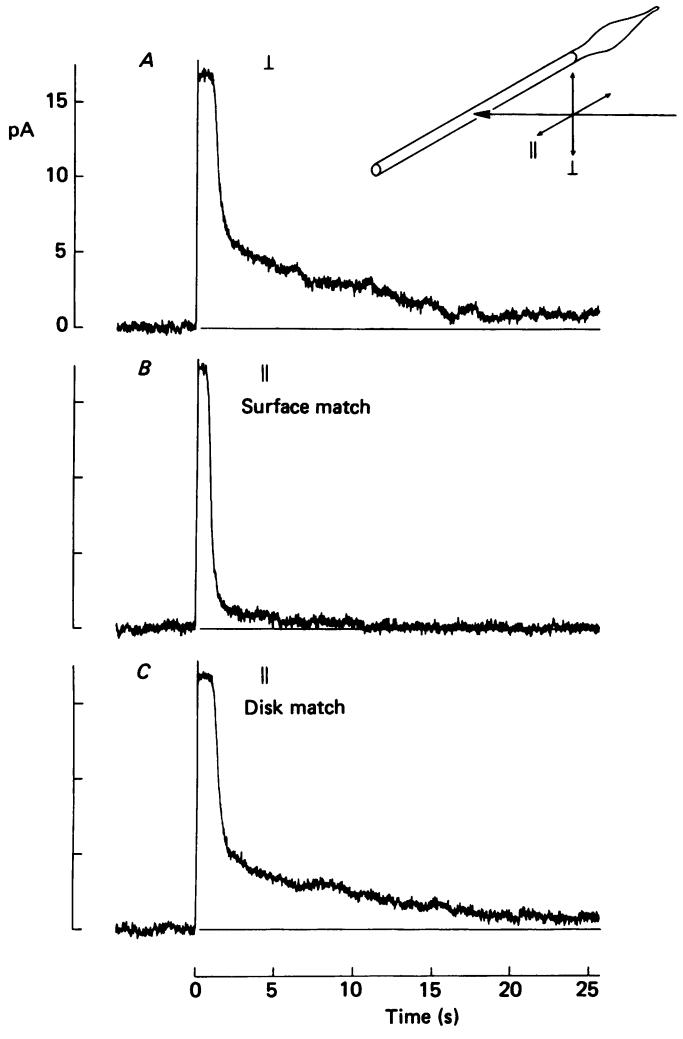

Fig. 12. Effect of plane of polarization on the magnitude of the tail current evoked by a flash. Each trace the average of four responses with the polarization perpendicular (⊥) or parallel (||) to the long axis of the rod (see inset). Flash strength in photons μm^{-2} (500 nm) was $1{\cdot}74 \times 10^3$ in *A*, $1{\cdot}28 \times 10^3$ in *B*, and $3{\cdot}98 \times 10^3$ in *C*. Absorption of light by rhodopsin in surface membrane approximately equal in *A* and *B*; absorption in disks approximately equal in *A* and *C*. Measured dichroic ratio 3·05. Band width 0–30 Hz; initial spike on photocurrent resulted from low-pass filtering. Temperature 36 °C. Cell 6 in Table 1.

photometry (see, e.g. Harosi, 1975), and the lower values here are explained by inexact alignment of the rod (see p. 577); the average value of $D = 2{\cdot}99$ is expected for an error of 17 deg.

Dependence of step length on longitudinal position of absorption in outer segment. After a toad rod is exposed to a bright diffuse flash the dark current recovers more slowly at the tip of the outer segment than at the base (Baylor & Lamb, 1982). This section

shows that a similar phenomenon occurs in primate rods and that it depends on differences in the kinetics of the step events.

Fig. 13*A* shows averaged responses from interleaved trials in which flashes were delivered locally on the tip or base of the outer segment; individual sweeps from this experiment are presented in Fig. 10. The photocurrent recovered more slowly after

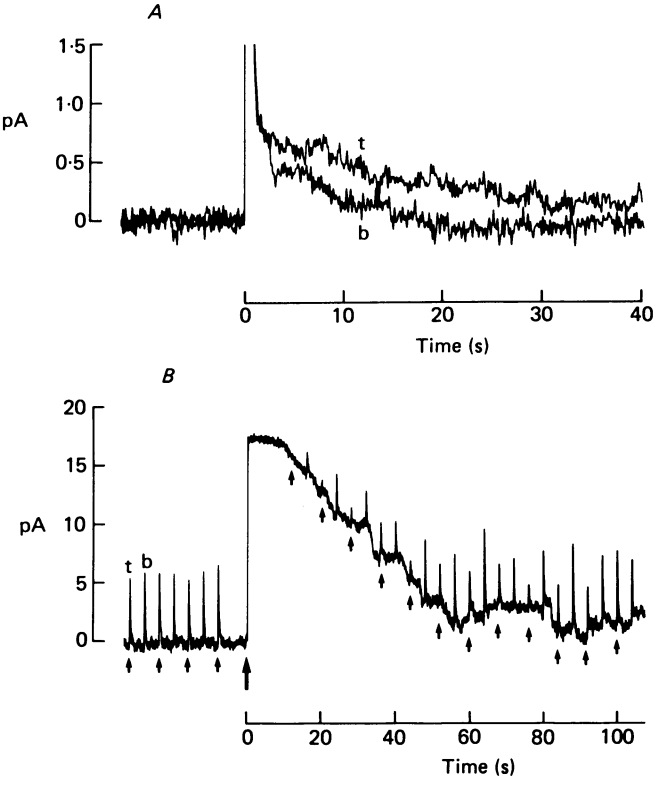

Fig. 13. Differences in recovery of tip and base after a bright flash. *A*, average responses to seventeen flashes at tip and fourteen flashes at base. Eight of the responses comprising the tip average shown in Fig. 10. Upper portion of photocurrent truncated. 520 nm light, 2·5 μm wide slit, $2{\cdot}1 \times 10^3$ photons μm^{-2}, approximately 250 isomerizations per flash. Temperature 36 °C, band width 0–5 Hz. Cell 5 in Table 1. *B*, recovery of flash sensitivity at tip and base after diffuse saturating flash. Diffuse flash indicated by bold arrow (500 nm light, $5{\cdot}6 \times 10^4$ photons μm^{-2}, about $9{\cdot}5 \times 10^4$ isomerizations). Flashes at tip and base; 10 μm slit, alternated in tip and base positions (tip flash indicated by small arrows). Light 520 nm, 88·6 photons μm^{-2}, giving about forty-two isomerizations per flash. Temperature 37 °C; band width 0–10 Hz.

flashes on the tip. The same result was obtained from measurements of the time between the flash and the fall of the last step in the individual sweeps. For the nine steps elicited from the tip the interval was $10{\cdot}2 \pm 5{\cdot}9$ s (mean $\pm$ S.D.), while for the nine steps from the base it was $6{\cdot}5 \pm 4{\cdot}2$ s. The stepped recovery lasted longer after flashes at the tip in each of four other runs on two other cells.

If a flash transiently increases the probability that a step will be generated, and

if a step lasts a variable time, the tip–base difference might arise from differences in the length of time during which a step may be generated or from differences in the mean length of a step. The limited number of trials do not allow this to be decided. Measured step lengths were roughly as expected for an exponential distribution with time constants of about 10 s, but larger samples are required for a proper test.

Fig. 13*B* shows results from an experiment to test the recovery of responsiveness at the tip and base of the outer segment after a bright flash (delivered at the large arrow). The flash was diffuse and bleached about 0·05 % of the rhodopsin. Test flashes were presented alternately at the tip and base of the outer segment, with the tip flashes indicated by the small arrows. As the dark current began to recover, flashes at the tip gave smaller responses than those at the base. This result would be expected if the steps at the tip lasted longer. Fluctuations in the responses to flashes at both positions presumably resulted from photon noise and fluctuations in the spatial distribution of the blocked regions. Similar results were obtained in each of three other runs on this cell.

Dark noise

In darkness the membrane current of toad rods shows a continuously present fluctuation of small amplitude as well as occasional 'discrete events' resembling single-photon responses (Baylor, Matthews & Yau, 1980). In analysing the dark noise of monkey rods we assume that it consists of two similar components.

Continuous component. Fig. 14*A* illustrates the reduction in current noise on illuminating a rod with saturating light. The current fluctuations in darkness were larger than those in saturating light. In bright light the noise variance fell to 0·054 pA^2 in the band 0–20 Hz. This can be compared with the variance σ_J^2 expected for Johnson noise in the electrode leakage resistance, by using the Nyquist relation

$$\sigma_J^2 = \frac{4kTb}{R}, \tag{9}$$

where k is Boltzmann's constant ($1{\cdot}38 \times 10^{-23}$ J K^{-1}), T is the absolute temperature (307 K), b is the recording band width (20 Hz), and R is the leakage resistance measured as 7·1 MΩ. The value of σ_J^2 calculated from eqn. (9) was 0·048 pA^2 in this experiment, similar to the measured variance in bright light. In an experiment on another cell the measured noise variance in the same band was 0·056 pA^2 in saturating light compared to the Johnson noise of 0·057 pA^2 calculated from the electrode resistance of 6·0 MΩ. In these experiments the noise observed in saturating light was therefore mainly instrumental, and the intrinsic cell noise can be estimated by subtracting the Johnson noise variance from the total dark variance.

The rod of Fig. 14 had a total dark variance of 0·067 pA^2 (0–20 Hz), giving an intrinsic variance of $0{\cdot}067 - 0{\cdot}048 = 0{\cdot}019$ pA^2. In seven such experiments, each on a different cell, the intrinsic variance estimated in this way was $0{\cdot}0288 \pm 0{\cdot}0089$ pA^2 (mean ± S.D.). The power spectrum of the intrinsic noise (dark spectrum minus saturating light spectrum) showed a low-pass filtered shape with a half-power frequency around 3 Hz (Fig. 14*B*). In all cells examined the intrinsic dark noise showed a spectrum of this general shape, with no noise measurable above the Johnson noise at frequencies greater than 5 Hz.

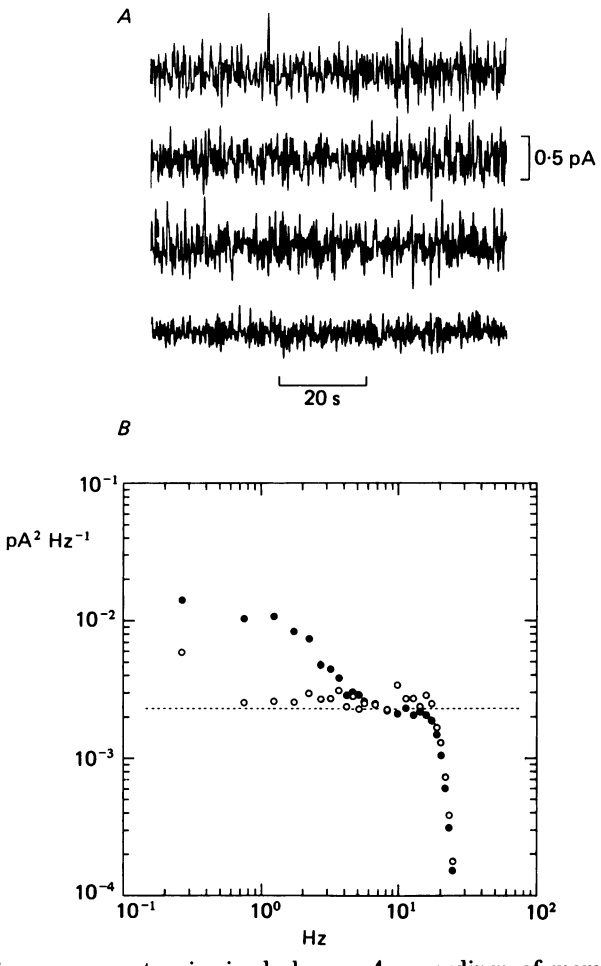

Fig. 14. Continuous current noise in darkness. *A*, recordings of membrane current in darkness (three upper traces) and in saturating light (lower trace). Band width 0·16–3 Hz. *B*, power spectral density of current fluctuations in darkness (●) and in saturating light (○) from the same rod. Dotted line drawn at the Johnson noise level for the measured electrode resistance of 7·1 MΩ. Dark spectrum calculated from eighteen sweeps of 20·48 s length, digitized at 100 Hz, with cosine tapering and linear trend removal. Spectral densities below 6 Hz were averaged over ten frequency points, above 6 Hz over thirty frequency points. Light spectrum calculated and plotted in same way from five sweeps. Saturating response 13 pA, t_{peak} 270 ms, HEPES buffer, 34 °C, band width 0–20 Hz.

Frequency of occurrence of discrete noise events in darkness. It was difficult to detect discrete noise events because the amplitude of the quantal current was not much larger than that of the background noise (continuous and instrumental). In order to estimate the frequency of occurrence, a series of dim flashes was given to determine the amplitude of the rod's single-photon response and then long recordings of current were made in darkness with the black box around the preparation completely closed. Under these conditions, there was no significant stray light in the box (Baylor *et al.* 1980).

In replaying the recordings for analysis, the band width was limited to 0·16–3 Hz (one-stage high-pass filter of 1 s time constant and six-pole low-pass filter at 3 Hz). The mean amplitude of the photon response was estimated from at least 100 responses to dim flashes as described previously, using either the histogram method or the ratio of ensemble variance and average. The dark record was digitized for determining its

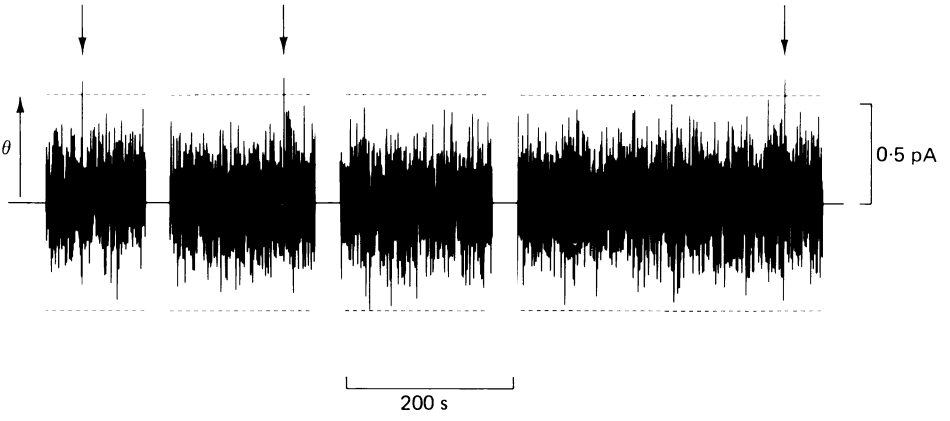

Fig. 15. 'Photon-like' noise events in darkness. Current in the band 0·16–3 Hz during a total record length of 700 s. During the gaps in the recording dim flashes were delivered for determining the amplitude of the single-photon effect. Dashed lines show the criterion level θ of 0·54 pA calculated to give false-positive counts at an expected rate of 2×10^{-3} s^{-1} (eqn. (10) in text). The estimated mean amplitude a of the quantal photocurrent was 0·7 pA in this rod in the band 0·16–3 Hz. Arrows above the record mark three crossings of the positive criterion level; no negative crossings occurred in this experiment. Dark variance 0·0217 pA^2, temperature 36 °C, electrode resistance with cell in place 5 MΩ. Cell 5 in Table 1.

variance and then played out at high gain on the inkwriter for counting the dark events. Results selected for analysis were from four cells that had a signal/noise ratio (mean photon response amplitude/standard deviation of dark noise) of more than 3·0. The dark record lengths ranged between 340 and 700 s.

The principle of the analysis was to select a criterion level that the background noise should rarely exceed and then to count the number of positive-going events above the criterion level (see Fig. 15). The level θ was selected for each experiment to give an arbitrary expected rate of false-positive events, ν, of 2×10^{-3} s^{-1}, as calculated from the variance σ^2 of the recording, using the expression (Rice, 1944; eqns. 3·3–12 and 3·3–14)

$$\nu = \frac{f_b}{\sqrt{3}} e^{-\theta^2/2\sigma^2}. \tag{10}$$

The band width f_b in eqn. (10) was taken as 3 Hz, ignoring the high-pass filtering. As a check on the analysis the number of negative-going events that exceeded a criterion of $-\theta$ was counted; this gave a total of three negative events compared to the four expected for the four experiments. The raw number of events above the criterion was corrected first for the expected number of false positives. A second

correction was then made to allow for photon-like events that did not exceed the criterion because of fluctuations in the base line and unit amplitude. This was done from a table of the cumulative normal distribution, assuming that the peak amplitude of the unit event was normally distributed, with a standard deviation equal to the square root of twice the total dark variance; this allows for a dispersion in the unit amplitude comparable to the base-line dispersion (see Table 3).

The total corrected number of events from all four experiments was 13·1, which for the total dark record length of 2067 s gave an estimated rate of $0{\cdot}0063 \pm 0{\cdot}0036$ s^{-1} (95 % confidence limits). The uncertainty in the estimate arises because the eleven events actually counted are drawn from a Poisson distribution with a standard deviation of roughly $\sqrt{11}$.

Evidence of a different kind for a low rate of photon-like events is present in the dark-amplitude histograms of Figs. 7*C* and *D* (insets). Each histogram shows a single event well outside the positive tail of the parent Gaussian distribution. The amplitudes of these events are similar to those of the cells' single photon responses. The total effective record length for the four experiments illustrated in Fig. 7 was 235 s. If only two events occurred during this period, the apparent rate is roughly similar to that from the previous method.

Baylor *et al.* (1980) measured quantal events in toad 'red' rods occurring at a rate of $0{\cdot}02$ s^{-1} at 20 °C. By correcting for rhodopsin content and temperature, they predicted in primate rods a quantal event rate of $0{\cdot}01$ s^{-1}, which is similar to that estimated here.

The derived rate of photon-like events allows one to set an upper limit on the rate constant for thermal isomerization of rhodopsin in the rod. Taking a figure of $1{\cdot}2 \times 10^8$ for the number of rhodopsin molecules in a rod, the rate constant is $0{\cdot}0063$ $s^{-1}/1{\cdot}2 \times 10^8 = 5{\cdot}2 \times 10^{-11}$ s^{-1}, corresponding to a half-life of 420 years.

DISCUSSION

Comparison with response of rods in other vertebrates

The saturating response amplitudes, flash sensitivities and half-saturating flash strengths reported here are similar to those reported by Penn & Hagins (1972), who made massed recordings from isolated retinas of the albino rat. The time scale and form of the response to dim flashes are also similar in the two studies. These points of agreement suggest that chopping the isolated monkey retina had little effect on the rods' flash responses. Penn & Hagins found background light to desensitize over a somewhat wider range, perhaps because they used flashes of constant strength to measure sensitivity while we adjusted the flash strength to evoke small linear responses.

The time scale and sensitivity of responses of toad rods are also similar to those described here if allowance is made for the different temperatures. A toad rod with $t_{peak} = 1$ s at 20 °C and a Q_{10} for $1/t_{peak}$ of 2·7 (Baylor, Matthews & Yau, 1983; Lamb, 1984) would have a t_{peak} of about 180 ms at 37 °C, comparable to that of the monkey rods. Conversely, in a few experiments at 20 °C the monkey rods showed dim-flash responses with t_{peak} near 1 s. In monkey rods the peak amplitude of the quantal current was about 0·7 pA at 37 °C. At 20 °C the quantal currents of toad rods are often near 1 pA but would be somewhat less at 37 °C (Baylor *et al.* 1983; Lamb, 1984).

Background light apparently desensitizes rods of toads and monkeys quite differently. In the primate rods there was little change in the kinetics of the incremental flash response and the main effects of backgrounds on flash sensitivity were predicted by the exponential saturation model of eqn. (8). Toad rods show an inverse relation between background intensity and flash sensitivity over at least two log units of background intensity (Fain, 1976; Baylor *et al.* 1980; Lamb *et al.* 1981), and the time scale of the incremental flash response shortens significantly as the background intensity rises.

During a toad rod's recovery from bright light the long tail current is accompanied by increased noise but steps are not evident (Lamb, 1980; Baylor & Lamb, 1982). If steps comprise the tail in toad rods, the underlying event must be smaller and/or briefer than that described here.

Processing of rod signals in the primate visual system

Kinetics. The integration time of the response to a dim flash was about 250 ms. A value of about 100 ms is measured in psychophysical experiments on the human scotopic system when a large spot is used; smaller spots give longer integration times (e.g. Barlow, 1957). The short perceptual integration time with large spots may depend partly on temporal high-pass filtering exerted after the photocurrent is generated. Indeed, voltage responses of turtle and salamander rods are high-pass filtered by voltage-sensitive conductance changes (Attwell & Wilson, 1980; Detwiler, Hodgkin & McNaughton, 1980; Baylor, Matthews & Nunn, 1984); additional high-pass filtering may be exerted during signal transfer at the retinal synapses (Baylor & Fettiplace, 1977; Schnapf & Copenhagen, 1982). A useful function of high-pass temporal filtering would be the suppression of error messages caused by step events in the rods (p. 593). If the photocurrent were analysed by a direct-coupled system a single step would be equivalent to a steady light causing about 5–10 photoisomerizations s^{-1} over the entire length of the step. Temporal differentiation would allow only the initial part of the spurious message to reach higher visual neurones.

Sites of background light effects in scotopic vision. It has been suggested that saturation of human scotopic vision corresponds to saturation in the rods themselves (Fuortes, Gunkel & Rushton, 1961; Adelson, 1982). In psychophysical experiments the saturation begins when the background light reaches about 100 scotopic td (Hayhoe, MacLeod & Bruch, 1976), or 528 photons μm^{-2} s^{-1} at the cornea for 500 nm light (Wyszecki & Stiles, 1967). Assuming a lens density of 0·160 (p. 584), the intensity at the retina would be 365 photons μm^{-2} s^{-1}. For a rod 2 μm in diameter, with an axial density of 0·35 at 500 nm (p. 584) and a quantum efficiency of isomerization of 0·67, the effective collecting area for axial illumination would be 1·16 μm^2. A stimulus of 100 scotopic td would therefore cause 423 isomerizations rod^{-1} s^{-1}. In comparison, the flash sensitivity for rods in bicarbonate fell to half in backgrounds causing about 100 photoisomerizations s^{-1}. The rough similarity in the two figures is probably consistent with the notion that human scotopic saturation occurs in the outer segments of the rods. Nevertheless, the difference in the intensities at which saturation begins is not explained.

The psychophysical increment threshold varies approximately linearly with background intensity when the background is between 0·002 and 100 scotopic td and

the conditioning and test spots are relatively large (Aguilar & Stiles, 1954). This behaviour has been interpreted as depending on a retinal gain control central to the rods (e.g. Rushton, 1965). The background light effects measured here support this interpretation inasmuch as the amplitude of the quantal current remained almost constant up to the equivalent of 10 scotopic td (42 photoisomerizations s^{-1}). At this level of background light the scotopic increment threshold, as measured by a large spot, rises by 10^4 times. Additional indirect evidence that moderate backgrounds do not desensitize the rods themselves comes from the psychophysical observation that the increment threshold measured with a small spot rises with approximately the square root of background intensity (Barlow, 1957). The form and scaling of this relation are explained if the rods register each photoisomerization and the background desensitizes only by causing photon noise.

Separation of single-photon effects from continuous noise in scotopic vision. The dark rate of discrete noise events was estimated to be 0·0063 s^{-1}. This is comparable to the psychophysical 'dark light' of about 0·01 s^{-1} (Aguilar & Stiles, 1954; Barlow, 1977), suggesting that the discrete events comprise the dark light. In the monkey rods, however, the dark noise was mainly composed of the continuous component. One way of expressing this is to give the equivalent rate of discrete events that would be required to produce the total variance observed in the dark. For a variance of 0·029 pA^2 (0–3 Hz), the equivalent rate, calculated by dividing the variance by the time integral of the squared quantal current, is 0·17 s^{-1}. Since the band widths of the continuous and discrete components are so similar, the continuous component would dominate the total noise after any linear operation on the rod current.

Assuming that the single-photon events and dark noise measured here are similar to those in the intact human eye, the correspondence between the psychophysical dark light and the discrete component suggests that in the scotopic system the continuous component is suppressed by a non-linear operation. One possibility would be a thresholding operation like that used for counting the discrete events in darkness (Fig. 15). Where should such an operation be performed? After optimum frequency filtering the amplitude a of the photon response was only about 4–5 times larger than the r.m.s. continuous noise, σ. When the outputs of N rods are pooled, the ratio of the quantal event amplitude to the r.m.s. noise will vary with $N^{-0.5}$. Therefore, for values of N approaching 10 the separation of quantal events from continuous noise would suffer severely. A reasonable location for the thresholding operation would be near the rods, perhaps at the synaptic relay to the second-order cells. An approximation to a thresholding operation might be achieved if there were a steep exponential dependence of synaptic transmitter release on the rod's membrane potential.

Spectral sensitivity

The peak spectral sensitivity of *Macaca* rods was estimated to be near 491 nm. This is close to the wave-length of maximal absorption of human rhodopsin in solution (493 nm, Wald & Brown, 1958; 494 nm, Bridges & Quilliam, 1973). Microspectrophotometry on single rod outer segments of *Macaca fascicularis* and man, however, gives estimates for the peak absorption that are red-shifted by several nanometres. For example, recent measurements on rods of *Macaca fascicularis* give λ_{max} as 500·1 ± 1·6 nm (Bowmaker *et al.* 1980) and 499·8 nm (MacNichol *et al.* 1983) and on

human rods 497·6 ± 3·3 nm (Bowmaker & Dartnall, 1980) and 496·3 ± 2·3 nm (Dartnall *et al.* 1983). A difference in the same direction has been noted for 'red' rods of *Bufo marinus*, which have a maximum sensitivity at 498 nm (Baylor *et al.* 1979*a*) and a maximum absorption at 501 nm (Harosi, 1975). A further difference between results obtained by the two methods is that the absorption spectrum measured by microspectrophotometry is broader than the action spectrum measured here and does not predict the observed form of the human scotopic sensitivity function (Bowmaker & Dartnall, 1980). The basis of these differences is not explained.

Supported by grant EY01543 from the National Eye Institute, USPHS. We thank Drs Carolyn Reed, Walter Makous and Trevor Lamb for assistance.

REFERENCES

ADELSON, E. H. (1982). Saturation and adaptation in the rod system. *Vision Research* **22**, 1299–1312.

AGUILAR, M. & STILES, W. S. (1954). Saturation of the rod mechanism at high levels of stimulation. *Optica Acta* **1**, 59–65.

ALPERN, M. & PUGH, E. N. (1974). The density and photosensitivity of human rhodopsin in the living retina. *Journal of Physiology* **237**, 341–370.

ATTWELL, D. & WILSON, M. (1980). Behaviour of the rod network in the tiger salamander retina mediated by membrane properties of individual rods. *Journal of Physiology* **309**, 287–315.

BADER, C. R., MACLEISH, P. R. & SCHWARTZ, E. A. (1979). A voltage-clamp study of the light response in solitary rods of the tiger salamander. *Journal of Physiology* **296**, 1–26.

BARLOW, H. B. (1957). Increment thresholds at low intensities considered as signal/noise discriminations. *Journal of Physiology* **136**, 469–488.

BARLOW, H. B. (1972). Dark and light adaptation: psychophysics. In *Handbook of Sensory Physiology*, vol. VII/4, *Visual Psychophysics*, ed. JAMESON, D. & HURVICH, L. M., pp. 1–28. New York: Springer Verlag.

BARLOW, H. B. (1977). Retinal and central factors in human vision limited by noise. In *Vertebrate Photoreception*, ed. BARLOW, H. B. & FATT, P., pp. 337–351. London: Academic.

BAYLOR, D. A. & FETTIPLACE, R. (1977). Kinetics of synaptic transfer from receptors to ganglion cells in turtle retina. *Journal of Physiology* **271**, 425–448.

BAYLOR, D. A. & HODGKIN, A. L. (1973). Detection and resolution of visual stimuli by turtle photoreceptors. *Journal of Physiology* **234**, 163–198.

BAYLOR, D. A., HODGKIN, A. L. & LAMB, T. D. (1974). The electrical response of turtle cones to flashes and steps of light. *Journal of Physiology* **242**, 685–727.

BAYLOR, D. A. & LAMB, T. D. (1982). Local effects of bleaching in retinal rods of the toad. *Journal of Physiology* **328**, 49–71.

BAYLOR, D. A., LAMB, T. D. & YAU, K.-W. (1979*a*). The membrane current of single rod outer segments. *Journal of Physiology* **288**, 589–611.

BAYLOR, D. A., LAMB, T. D. & YAU, K.-W. (1979*b*). Responses of retinal rods to single photons. *Journal of Physiology* **288**, 613–634.

BAYLOR, D. A., MATTHEWS, G. & NUNN, B. J. (1984). Location and function of voltage-sensitive conductances in retinal rods of the salamander *Ambystoma tigrinum*. *Journal of Physiology* **354**, 203–223.

BAYLOR, D. A., MATTHEWS, G. & YAU, K.-W. (1980). Two components of electrical dark noise in toad retinal rod outer segments. *Journal of Physiology* **309**, 591–621.

BAYLOR, D. A., MATTHEWS, G. & YAU, K.-W. (1983). Temperature effects on the membrane current of retinal rods of the toad. *Journal of Physiology* **337**, 723–734.

BLOUGH, D. S. & SCHRIER, A. M. (1963). Scotopic spectral sensitivity in the monkey. *Science* **149**, 493–494.

BOWMAKER, J. K. & DARTNALL, H. J. A. (1980). Visual pigments of rods and cones in a human retina. *Journal of Physiology* **298**, 501–511.

BOWMAKER, J. K., DARTNALL, H. J. A. & MOLLON, J. D. (1980). Microspectrophotometric demonstration of four classes of photoreceptor in an old world primate *Macaca fascicularis*. *Journal of Physiology* **298**, 131–143.

BRIDGES, C. D. B. & QUILLIAM, T. A. (1973). Visual pigments of men, moles and hedgehogs. *Vision Research* **13**, 2417–2421.

CRAWFORD, B. H. (1949). The scotopic visibility function. *Proceedings of the Physical Society* **B62**, 321–334.

DARTNALL, H. J. A. (1972). Photosensitivity. In *Photochemistry of Vision*, ed. DARTNALL, H. J. A., pp. 122–145. New York: Springer Verlag.

DARTNALL, H. J. A., BOWMAKER, J. K. & MOLLON, J. D. (1983). Human visual pigments: microspectrophotometric results from the eyes of seven persons. *Proceedings of the Royal Society* B **220**, 115–130.

DETWILER, P. B., CONNER, J. D. & BODOIA, R. D. (1982). Gigaseal patch clamp recordings from outer segments of intact retinal rods. *Nature* **300**, 59–61.

DETWILER, P. B., HODGKIN, A. L. & MCNAUGHTON, P. A. (1980). Temporal and spatial characteristics of the voltage response of rods in the retina of the snapping turtle. *Journal of Physiology* **300**, 213–250.

DEVALOIS, R. L., MORGAN, H. C., POLSON, M. C., MEAD, W. R. & HULL, E. M. (1974). Psychophysical studies of monkey vision. I. Macaque luminosity and color vision tests. *Vision Research* **14**, 53–67.

FAIN, G. L. (1976). Sensitivity of toad rods: dependence on wavelength and background illumination. *Journal of Physiology* **261**, 71–101.

FUORTES, M. G. F., GUNKEL, R. D. & RUSHTON, W. A. H. (1961). Increment thresholds in a subject deficient in cone vision. *Journal of Physiology* **156**, 179–192.

FUORTES, M. G. F. & YEANDLE, S. (1964). Probability of occurrence of discrete potential waves in the eye of *Limulus*. *Journal of General Physiology* **47**, 443–463.

HAGINS, W. A., PENN, R. D. & YOSHIKAMI, S. (1970). Dark current and photocurrent in retinal rods. *Biophysical Journal* **10**, 380–412.

HAYHOE, M. M., MACLEOD, D. I. A. & BRUCH, T. A. (1976). Rod-cone independence in dark adaptation. *Vision Research* **16**, 591–600.

HAROSI, F. I. (1975). Absorption spectra and linear dichroism of some amphibian photoreceptors. *Journal of General Physiology* **66**, 357–382.

HECHT, S., SHLAER, S. & PIRENNE, M. H. (1942). Energy, quanta, and vision. *Journal of General Physiology* **25**, 819–840.

KATZ, B. & MILEDI, R. (1972). The statistical nature of the acetylcholine potential and its molecular components. *Journal of Physiology* **224**, 665–699.

LAMB, T. D. (1980). Spontaneous quantal events induced in toad rods by pigment bleaching. *Nature* **287**, 349–351.

LAMB, T. D. (1984). Effects of temperature changes on toad rod photocurrents. *Journal of Physiology* **346**, 557–578.

LAMB, T. D., MCNAUGHTON, P. A. & YAU, K.-W. (1981). Spatial spread of activation and background desensitization in toad rod outer segments. *Journal of Physiology* **319**, 463–496.

MACNICHOL, E. F., LEVINE, J. S., LIPITZ, L. E., MANSFIELD, R. J. W. & COLLINS, B. A. (1983). Microspectrophotometry in primate photoreceptors. In *Colour Vision: Physiology and Psychophysics*, ed. MOLLON, J. D. & SHARPE, L. T., pp. 13–38. London: Academic Press.

MORGAN, A. A. (1966). Chromatic adaptation in the macaque. *Journal of Comparative and Physiological Psychology* **62**, 76–83.

NAKA, K. I. & RUSHTON, W. A. H. (1966). S-potentials from colour units in the retina of fish (*Cyprinidae*). *Journal of Physiology* **185**, 536–555.

NUNN, B. J. & BAYLOR, D. A. (1982). Visual transduction in retinal rods of the monkey, *Macaca fascicularis*. *Nature* **229**, 726–728.

NUNN, B. J. & BAYLOR, D. A. (1983). Visual transduction in rods of the monkey, *Macaca fascicularis*. In *Color Vision: Physiology and Psychophysics*, ed. MOLLON, J. D. & SHARPE, L. T., pp. 1–11. London: Academic Press.

NUNN, B. J., SCHNAPF, J. L. & BAYLOR, D. A. (1984). Spectral sensitivity of single cones in the retina of the monkey, *Macaca fascicularis*. *Nature* **309**, 264–266.

PENN, R. D. & HAGINS, W. A. (1972). Kinetics of the photocurrent of retinal rods. *Biophysical Journal* **12**, 1073–1094.

RICE, S. O. (1944). Mathematical analysis of random noise. *Bell System Technical Journal*, vol. 23, pp. 282–332; vol. 24, pp. 44–156. Reprinted in *Selected Papers on Noise and Stochastic Processes*, ed. WAX, N. New York: Dover, 1954.

RUSHTON, W. A. H. (1965). Visual adaptation. The Ferrier Lecture, 1962. *Proceedings of the Royal Society* B **162**, 20–46.

SCHNAPF, J. L. (1983). Dependence of the single photon response on longitudinal position of absorption in toad rod outer segments. *Journal of Physiology* **343**, 147–159.

SCHNAPF, J. L. & COPENHAGEN, D. R. (1982). Differences in the kinetics of rod and cone synaptic transmission. *Nature* **296**, 862–864.

SCHOLES, J. (1965). Discontinuity of the excitation process in locust visual cells. *Cold Spring Harbor Symposia on Quantitative Biology* **XXX**, 517–527.

WALD, G. & BROWN, P. K. (1958). Human rhodopsin. *Science* **127**, 222–226.

WYSZECKI, G. & STILES, W. S. (1967). *Color Science*. New York: Wiley.

ZWAS, F. & ALPERN, M. (1976). The density of human rhodopsin in the rods. *Vision Research* **16**, 121–127.